



**UNIVERSITÀ DEGLI STUDI DI PALERMO**  
**SCUOLA POLITECNICA**

Dipartimento di Energia, ingegneria dell'Informazioni e modelli Matematici  
Corso di Laurea Magistrale in Ingegneria Elettronica

**MICROCONTROLLER BASED  
ENGINE CONTROL UNIT**

TESI DI LAUREA DI  
**JORDI PRIETO BOLINCHES**

Matricola: 0662457

RELATORE  
**PROF. G. COSTANTINO GIACONIA**

**PROF. EMILIANO PIPITONE**

ANNO ACCADEMICO 2016 - 2017

---

MAGISTRALE





# Contents

<b>Contents</b>	<b>3</b>
<b>List of Figures</b>	<b>6</b>
<b>Abstract</b>	<b>9</b>
<b>Resumen</b>	<b>11</b>
<b>1 Introduction</b>	<b>13</b>
1.1 Motivations of the proposed work . . . . .	13
1.2 Objectives . . . . .	13
1.3 Final Report organization . . . . .	14
<b>2 Theoretical foundations</b>	<b>15</b>
2.1 Introduction . . . . .	15
2.2 Fundamentals of Reciprocating Engines . . . . .	15
2.2.1 Method of operation . . . . .	16
2.2.2 Spark ignition engine (SI engine) . . . . .	17
2.2.3 Compression ignition engine (CI engine) . . . . .	19
2.2.4 Differences between Compression Ignition and Spark Ignition Engines . . . . .	22
2.3 LPG-Diesel Fuel Engine . . . . .	24

2.3.1	HCCI Engine . . . . .	25
2.3.2	SCCI Engine . . . . .	25
2.4	Fuel Injection System . . . . .	27
2.4.1	Fuel injector for intake-manifold injection . . . . .	27
2.4.2	Common-rail system . . . . .	29
2.4.2.1	Common-rail diesel injectors . . . . .	31
2.5	Engine Control Unit . . . . .	33
<b>3</b>	<b>Specifications and Technologies required</b>	<b>35</b>
3.1	Introduction . . . . .	35
3.2	KOHLER Diesel KDI 1903 TCR Engine . . . . .	36
3.2.1	Engine specifications . . . . .	36
3.2.2	Fuel Injection System . . . . .	37
3.3	Digital intelligence . . . . .	38
3.3.1	STM32 NUCLEO-F401RE Development Board . . . . .	38
3.3.1.1	General-purpose I/Os (GPIOs) . . . . .	40
3.3.1.2	Timers and counters . . . . .	42
3.3.1.3	ST-LINK/V2 debugger and programmer . . . . .	43
3.3.1.4	Analog-to-digital converter . . . . .	43
3.3.2	STM32Cube . . . . .	45
3.3.3	System Workbench for STM32 (SW4STM32) . . . . .	47
3.3.4	System development environment NI LabVIEW . . . . .	48
3.3.4.1	Execution structures . . . . .	48
3.3.4.2	VISA Functions . . . . .	49
3.4	Injection system control . . . . .	51
3.4.1	Control sequence of diesel injectors . . . . .	51
3.4.2	Boost converter Voltage . . . . .	52
3.4.3	Boost Converter . . . . .	53

<i>CONTENTS</i>	5
<b>4 Experimental results</b>	<b>57</b>
4.1 Introduction . . . . .	57
4.2 Power Stage Design . . . . .	57
4.2.1 General Electrical Schematic of the injection system . . . . .	58
4.2.2 Diagram of the gas injection system . . . . .	58
4.2.3 Diesel injection system . . . . .	59
4.2.3.1 Control design of the Boost Converter . . . . .	60
4.2.3.2 Supply voltage selection . . . . .	62
4.2.3.3 Current reading of the diesel injectors . . . . .	65
4.2.4 Selection of the injectors . . . . .	66
4.2.5 Acquisition of the trigger signal . . . . .	67
4.3 Microcontroller program . . . . .	68
4.3.1 Calculation of the injection position . . . . .	69
4.3.2 Communication with the PC . . . . .	73
4.4 Virtual Instrument (LabVIEW) . . . . .	74
4.5 Experimental measurements . . . . .	75
4.5.1 Conventional Diesel Fuel Injection . . . . .	75
4.5.1.1 Diesel injection controlled by the designed ECU . . . . .	76
4.5.2 LPG-Diesel Fuel Injection . . . . .	77
<b>5 Conclusion</b>	<b>81</b>
<b>Bibliography</b>	<b>83</b>

# List of Figures

2.1	Working cycle of the 4 stroke engine, [6]	16
2.2	Ideal air standard Otto cycle in a p, V diagram, [10]	18
2.3	Conceptual schematic of conventional diesel combustion, showing the contamination regions, [3]	20
2.4	The Sabathé cycle in a p, V diagram, [10]	22
2.5	Formation regions of NO <sub>x</sub> and soot in a $\phi$ - T diagram, [9]	24
2.6	Intake Manifold Electromagnetic Fuel Injector, [12]	27
2.7	Injection-duration correction according to the battery voltage, [12]	28
2.8	Injection-duration correction according to the battery voltage, [12]	29
2.9	Diagram of the common-rail system, [11]	30
2.10	Diagram of the common-rail system, [11]	31
2.11	Main components of EDC, [11]	33
3.1	KDI 1903 TCR Performance Curves, [7]	37
3.2	STM32 NUCLEO-F401RE development board, [18]	38
3.3	Summary of the main features of the STM32F401xD/xE microcontrollers, [13]	40
3.4	Block diagram of the STM32F401xD/xE microcontrollers, [16]	41
3.5	Features of STM32F401RE timers, [16]	42
3.6	Characteristic times of the ADC converter.	45
3.7	Overview of STM32CubeMX C code generation flow, [20]	46

3.8	STM32CubeMX main window . . . . .	47
3.9	While Loop . . . . .	49
3.10	Case Structure . . . . .	49
3.11	VISA Configure Serial Port Diagram . . . . .	50
3.12	VISA Write Function Diagram . . . . .	50
3.13	VISA Read Function Diagram . . . . .	50
3.14	VISA Close Function Diagram . . . . .	50
3.15	Diesel fuel injection sequence, [11] . . . . .	51
3.16	Injector currents at different voltages . . . . .	53
3.17	Boost Converter diagram . . . . .	54
3.18	Equivalent circuit with the switch closed (MOSFET ON) . . . . .	54
3.19	Equivalent circuit with the switch open (MOSFET OFF) . . . . .	55
4.1	Conceptual diagram of the injector system . . . . .	57
4.2	General Electrical Schematic of the injection system . . . . .	58
4.3	Gas Injection Schematic . . . . .	59
4.4	Diesel Injection Schematic . . . . .	59
4.5	Boost Converter Circuit . . . . .	60
4.6	Timing Resistor ( $R_T$ ) Value, [8] . . . . .	61
4.7	Maximum SENSE Threshold Voltage vs Duty Cycle, [8] . . . . .	62
4.8	High Side Mosfet Driver . . . . .	63
4.9	Voltage difference between Source and Gate on the IRFP9140N transistor . . . . .	64
4.10	AD8207 Schematic. Ground Referenced Output Mode, $V_+ = 5V$ , [1] . . . . .	66
4.11	Low Side MOSFET driver . . . . .	67
4.12	Conditioning of Trigger Signal . . . . .	68
4.13	Main Flow Diagram . . . . .	69
4.14	Diesel Injection Diagram . . . . .	70
4.15	Current Control Diagram . . . . .	71

4.16	Communication Diagram . . . . .	73
4.17	Front Panel of the Virtual Instrument . . . . .	74
4.18	Solenoid-valve current (100 mV/A) . . . . .	75
4.19	Solenoid current controlled by designed ECU (100 mV/A) . . . . .	76
4.20	Solenoid-valve current (100 mV/A) . . . . .	77
4.21	LPG injection at 2000 rpm . . . . .	78
4.22	Diesel injection at 2000 rpm . . . . .	78
4.23	Separation between diesel injections (2000 rpm) . . . . .	79
4.24	Solenoid-valve current controlled by designed ECU (100 mV/A) . . . . .	79



# Abstract

This work is devoted to the design and implementation of an Engine Control Unit (ECU) for the management of a LPG-Diesel dual-fuel engine. The ECU is implemented by using a STM32 Nucleo board equipped with the Cortex M4 based (STM32F401) microcontroller, being able to control the engine, whether it works in conventional diesel mode or in a dual fuel combustion fashion.

In order to reach this goal a tailored daughter board, attached to the Arduino-compatible I/O pins available on the STM32 Nucleo, has been designed and built. Its main function is to act as a driver and a final stage, capable to generate the proper outputs for the engine under test.

In both operation modes (single and dual fuel combustion) , the embedded system will be able to sample some relevant parameters such as phase synchronization signal and crankshaft engine signal and to control, with high degree of flexibility due to the microcontroller firmware, the time and the shape of injection signals and the amount of fuel delivered at each cycle.

Finally, the system may work as a standalone application or as a slave element, controlled by a purposely designed software running as a LabVIEW application through a remote personal computer.



# Resumen

Este trabajo se dedica al diseño e implementación de una Unidad de Control de Motor (ECU) para el manejo de un motor de doble combustible GLP-Diésel. La ECU está implementada empleando la tarjeta de desarrollo STM32 Nucleo equipada con el microcontrolador STM32F401, basado en Cortex M4, siendo capaz de controlar el motor, tanto si funciona en modo diésel convencional como en modo doble combustible.

Para alcanzar este objetivo se ha diseñado y construido una tarjeta unida mediante los pines I/O compatibles con Arduino disponibles en la STM32 Nucleo. Su función principal es actuar como controlador y etapa final, siendo capaz de generar las salidas apropiadas para el motor sometido a ensayo.

En ambos modos de operación (combustión simple y dual fuel) el sistema embebido es capaz de obtener algunos parámetros relevantes tales como las señales de sincronización de fase y del ángulo del cigüeñal y controlar, con un alto grado de flexibilidad debido al firmware del microcontrolador, el tiempo y la forma de las señales de inyección, además de la cantidad de combustible entregada en cada ciclo.

Finalmente, el sistema puede funcionar como una aplicación independiente o como un elemento esclavo, controlado por una aplicación diseñada con LabVIEW en un ordenador personal remoto.



# **1 Introduction**

## **1.1 Motivations of the proposed work**

One of the biggest challenges that progress gives to our contemporary life is to control the emission of polluting gases from human activities, causing the greenhouse effect and worsening of health conditions. The main sources of these gases are the burning of fossil fuels, used mainly in industry and transport, agriculture and livestock sectors.

The diesel is one of the most used fuels due to its versatility and price, but it is also one of the most harmful for the environment because it is a source of soot (harmful to the respiratory system and potentially carcinogenic) and oxides of nitrogen, gases behind global warming. It also generates other corrosive compounds, such as tropospheric ozone.

For these reasons, the use of alternative fuels such as biodiesel, ethanol or liquid petroleum gas (LPG) is being studied. This project is focused on the latter to develop a control of a SCCI engine, a dual-fuel LPG-Diesel engine.

## **1.2 Objectives**

The main objective of the present work is to design and implement an Engine Control Unit, for the management of a dual fuel LPG-Diesel engine, capable to jointly use LPG and diesel as a fuels. The motivation of this simultaneous use, is to reduce the  $\text{NO}_x$  and soot emissions characteristics of the conventional combustion process of diesel engines.

The design of the control unit has been made in two parts: the digital intelligence and the control circuit.

As digital intelligence it has been used a STM Nucleo board, based on ARM Cortex M4, specifically the STM32F401 microcontroller. It has been possible to manage the two desired modes of operations: diesel conventional and dual fuel.

The control circuit has been designed as an interface between the digital logic and the engine by implementing a card, connected to the Arduino compatible inputs and outputs of the STM32 Nucleo board. This board drives the injectors and by obtaining certain relevant parameters, such as the current provided or the speed and angle of the crankshaft, necessary to calculate the precise moment of the injections.

### **1.3 Final Report organization**

This report is arranged with the following sections:

- In the first one, the theoretical foundations needed for the project are discussed. Reciprocating Engines and dual-fuel modifications are defined, together with the basic equipment and processes of these thermal machines, such as the ECU or the fuel injection system.
- The second part focuses on the used equipment and the elements needed to perform the digital logic.
- Finally the third chapter describes the power stage design, the microcontroller software, the virtual instrument, designed with LabVIEW, and the experimental results are presented.

## **2 Theoretical foundations**

### **2.1 Introduction**

In this chapter the theoretical foundations of the most common Reciprocating Engines (Spark and Compression ignition) are presented, and how the dual fuel engine has been obtained from them. The injection system and its control will be also exposed.

### **2.2 Fundamentals of Reciprocating Engines**

The engines are mechanic systems in charge to transform some type of energy in mechanical energy. Among them, we find the heat engine that uses the chemical energy present in a combustible material as source of heat. Depending on the place where the combustion takes place, they are classified in external and internal combustion engines, with the reciprocating engine laying within the second group.

In a reciprocating engines, the pressure of the gases mixture resulting from the combustion process pushes a piston into its cylinder and, through a connecting rod, the crankshaft is rotated, thus obtaining a rotational movement. They can be classified according to non-exclusive criteria among them, such as the combustion process, fuel type or air and fuel introduction systems. In the present project, we classified them according to their combustion process, in spark ignition and compression engine.

### 2.2.1 Method of operation

The reciprocating engines, whether CI or SI, can be classified in four-stroke or two-stroke engines depending on the revolutions by cycle of the crankshaft, [6, 10, 12].

#### Four-stroke operating cycle

The majority of the reciprocating engines use a four-stroke cycle (see Fig. 2.1). This means that the engine needs two revolutions of the crankshaft for complete the work sequence.

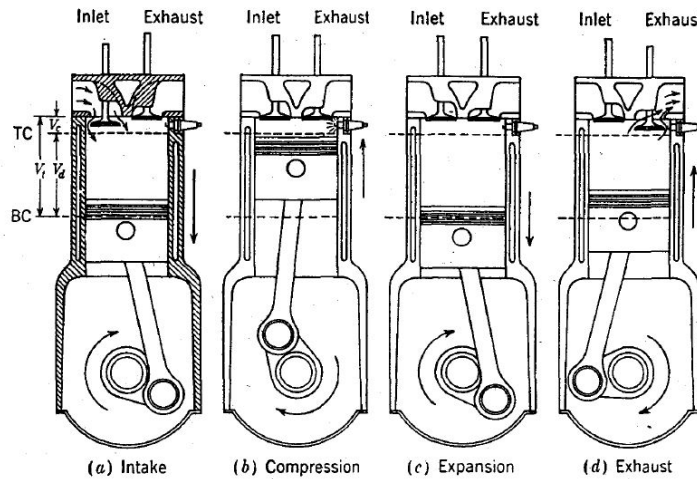


Figure 2.1: Working cycle of the 4 stroke engine, [6]

- a. Intake stroke: When the piston is in the Top Dead Center (TDC), it begins to move towards the Bottom Dead Center (BDC). The volume into the cylinder increase, absorbing an air-fuel mixture or air only, depending on whether the engine works with homogeneous or stratified mixture, respectively. When it reaches the BDC, the inlet valves close.
- b. Compression stroke: During the second stroke, the piston moves towards the TDC, compressing the air or mixture during its travel, thus increasing its temperature.



Near the TDC, combustion is initiated, rising the internal cylinder pressure.

- c. Expansion stroke: The high pressure pushes the piston toward the BDC, forcing the crankshaft to rotate.
- d. Exhaust stroke: Moments before reaching the BDC, the exhaust valves open and, by inertia, the piston push the burned gases to the outside during its ascent.

### 2.2.2 Spark ignition engine (SI engine)

The spark ignition engines, also known as Otto engine in honor of its inventor, is an internal combustion engine where the combustion process is ignited by an external energy input, like an spark plug. This system allows to choose the ideal moment to start the combustion for improve the efficiency.

The addition of the fuel can be performed in two ways: indirect or homogeneous, where the fuel has been mixed with the air before the introduction in the cylinder; and direct or stratified, where the air is first introduced into the engine and, during the compression stroke, the fuel is added, [10].

#### Formation of the air-fuel mixture

In SI engines the use of injections systems is common. The injector can be located in both the inlet manifold and the cylinder. In the first case, the injection is performed during the intake stroke, giving enough time to prepare a homogeneous mixture. In the second, the injection can be performed both during the intake and compression stroke, changing the time available in each case, [10].

These engines work with a lambda ratio ( $\lambda$ ) close to the unit, in other words, close the stoichiometric or ideal value (14.7 kg of air for 1 kg of fuel), [12]. The lambda ratio indicates the deviation of the amount of air introduced with respect to the ideal:

$$\lambda = \frac{\text{air mass introduced}}{\text{mass of air required}} \quad (2.1)$$

If the amount of fuel relative to the air is decreased ( $\lambda > 1$ ), a lean mixture is obtained. Near the stoichiometric value, the specific fuel consumption and the CO emissions decrease, at the expense of lose power. On the other hand, a rich mixture ( $\lambda < 1$ ) increase the power, increasing in turn pollution and consumption. Thus, this last form is only used to start a cold engine or to make a strong acceleration.

### Otto cycle

The Otto cycle is an ideal air standard cycle. This means that is a simplification of the real cycle, used for predict some parameters like work or efficiency.

This cycle is usually used to explain the operation in spark ignition engines. It consists of four processes, as shown in Fig. 2.2:

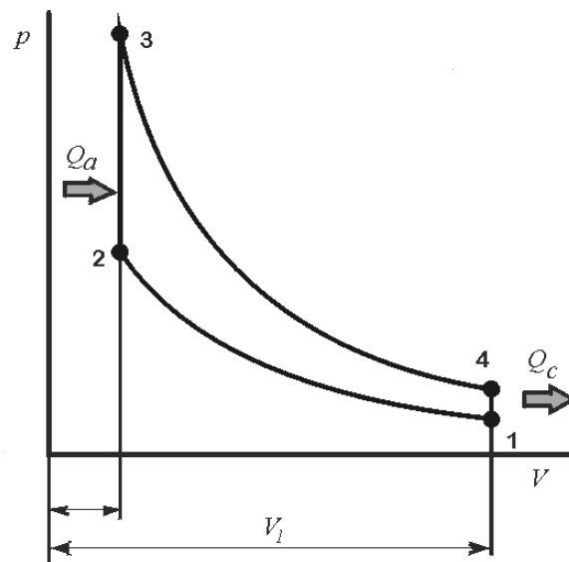


Figure 2.2: Ideal air standard Otto cycle in a p, V diagram, [10]

- 1-2 Isentropic compression ( $\Delta S = 0$ ). The pressure inside the cylinder increases while the volume decrease without a heat exchange.
- 2-3 Heat addition ( $Q_a$ ) at constant volume. The air/fuel mixture burns, increasing the pressure but keeping volume constant.
- 3-4 Isentropic expansion ( $\Delta S = 0$ ). The volume increase while the pressure decrease without a heat exchange.
- 4-1 Heat rejection ( $Q_c$ ) at constant volume, completing the cycle.

### 2.2.3 Compression ignition engine (CI engine)

The compression ignition engine, also known as diesel engine, in honor of its inventor, Rudolf Diesel, is the other most common type of reciprocating engine. It produces the movement due to the autoignition of the mixture formed by fuel and air caused by the high pressure inside the cylinders. The typical process is the following: the air temperature rises due to the compression process and, in the maximum pressure/temperature point, the fuel is introduced, which ignites when makes contact with the air.

The first diesel engines did not have the capacity to compress the fuel, which made it necessary to use a compressed air to sweep along it into the combustion chamber. The principal problem of this procedure is that it was not suitable for high loads or speeds, because this results in local over-enrichments due to a deficient dispersion, causing a significant increase in the smoke emissions.

The next development was the use of a precombustion chamber interconnected with the main chamber by small bores. This system eliminated the need to use the air compressor, reducing the weight and size of the engine. This mechanism, which is still used today in some systems, consists in introducing the whole amount of fuel at high pressure in the small chamber, about one-fifth the size of the main chamber. Due to the small quantity of

air present, only little part of it self-ignites, causing an increase in the pressure that forces the mixture to move to the main chamber, [11].

Nowadays, this last process has been practically replaced in all the engines. The fuel is now injected directly inside the cylinder, allowing to control both the moment and the amount of fuel injected, thus improving the efficiency and, consequently, obtaining a considerable reduction in the emission of polluting gases.

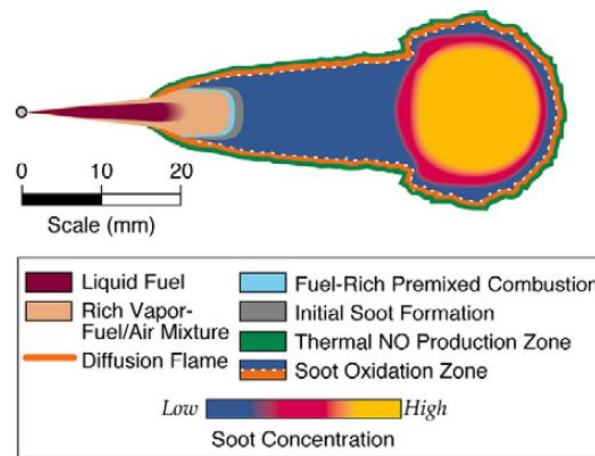


Figure 2.3: Conceptual schematic of conventional diesel combustion, showing the contamination regions, [3]

Since the combustion starts while the fuel begins to enter into the chamber, the air-fuel mixture is very heterogeneous, producing different flame fronts throughout the injection at those points where the dosage is close to the stoichiometric value. This generates efficiency losses and increase of the emissions, in the regions that can be observed in Fig. 2.3.

With the objective to reduce the emissions, in recent years several modifications to conventional operation have been proposed. One of these modifications is the HCCI engine (Homogeneous Charge Compression Ignition), and its derivate SCCI (Stratified Charge Compression Ignition), exposed in section 2.3.

### Formation of the air-fuel mixture

In CI engines that utilize direct injection, the fuel is always injected, in one or several times, at high pressure when the piston is near the Top Dead Center, creating the mixture inside the cylinder. The injection system has to be able to spread the fuel and mix it quickly with the air.

These engines work with a lambda ratio ( $\lambda$ ) superior to the unit, in other words, they work with more air than required. The stoichiometric or ideal value is 14.5 for a diesel fuel (14.5 kg of air for 1 kg of fuel), [11]. The lambda ratio indicates the deviation of the amount of air introduced with respect to the ideal:

$$\lambda = \frac{\text{air mass introduced}}{\text{mass of air required}} \quad (2.2)$$

The lambda ratio for turbocharged diesel engines is  $\lambda > 10$  under no-load conditions and between 1.15 and 2 at full load, [11].

### Sabathé cycle

The Sabathé cycle (also known as Seiliger cycle) is the air standard cycle that best represents the combustion process in the compression ignition engines. It is, like the Otto cycle, a simplification of the real cycle, used for predict some parameters like work or efficiency.

With this cycle we can to explain the operation in compression ignition engines, that consists of five processes, as shown in Fig. 2.4:

- 1-2 Isentropic compression ( $\Delta S = 0$ ). The pressure inside the cylinder increases while the volume decrease without a heat exchange.
- 2-3 Heat addition ( $Q_a$ ) at constant volume. The air/fuel mixture starts to burn, increasing the pressure but keeping volume constant.

3-3' Heat addition ( $Q_a$ ) at constant pressure. The piston starts to move, keeping the pressure constant. The mixture is still burning.

3'-4 Isentropic expansion ( $\Delta S = 0$ ). The combustion is complete. The volume increases while the pressure decreases without a heat exchange.

4-1 Heat rejection ( $Q_c$ ) at constant volume, completing the cycle.

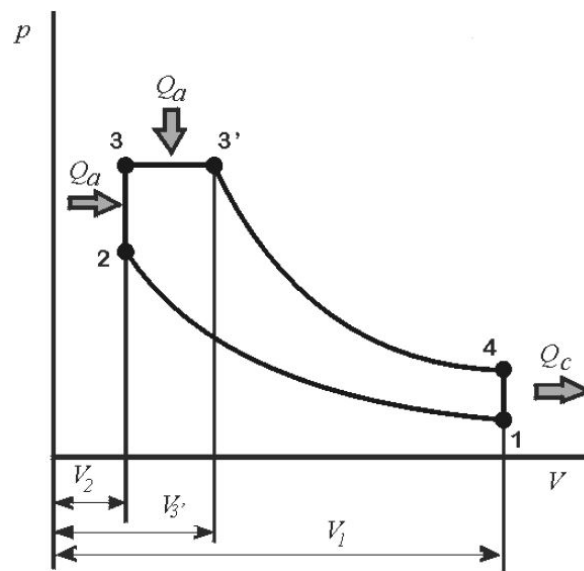


Figure 2.4: The Sabathé cycle in a  $p, V$  diagram, [10]

## 2.2.4 Differences between Compression Ignition and Spark Ignition Engines

Summarizing the sections 2.2.2 and 2.2.3, the main difference between the two engines, as can be deduced from the names, is their ignition process, that depends on the mixture characteristics.

The Compression Ignition engines require high temperature inside the cylinders for their proper functioning. Because of this, the air fuel mixture cannot be introduced until the right time in order to avoid an anticipated spontaneous ignition.

In the Spark Ignition engines the situation is the opposite: the air fuel mixture is introduced at the beginning of the admission stroke. This is because a homogeneous mixture is needed to make a correct combustion. As the combustible is within the chamber during the compression stroke, the working temperature must be below the autoignition point of the mixture to avoid premature detonations, which generate noise, performance losses and even an engine breakdown.

## 2.3 LPG-Diesel Fuel Engine

As mentioned in the Sec. 2.2.3, in order to reduce the problems of performance losses and pollution in the engines that work with a very heterogeneous or stratified mixture, some modifications have been applied in the air and fuel intake processes. But first, to better explain the modifications made in the engine, we are going to explain the reasons why the use of a stratified mixture causes a high contaminating gases emissions.

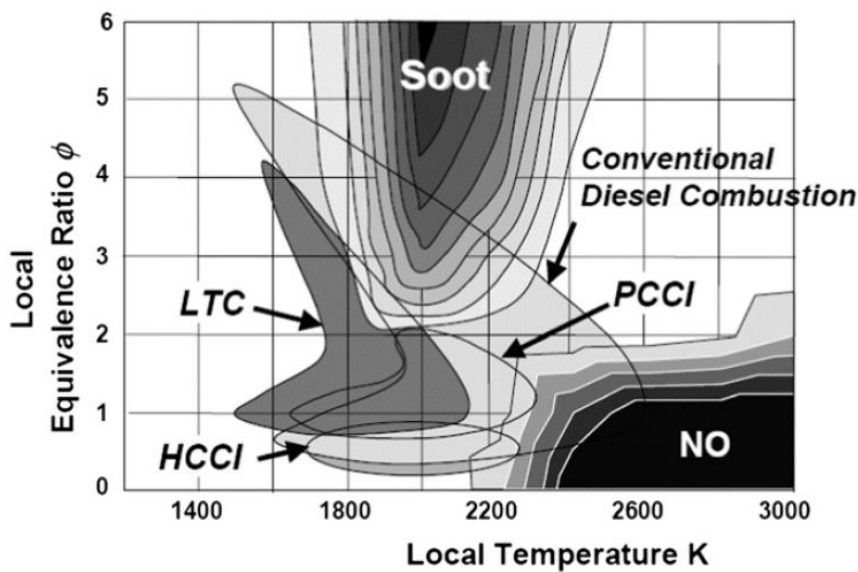


Figure 2.5: Formation regions of NO<sub>x</sub> and soot in a  $\phi$  - T diagram, [9]

As shown in the Fig. 2.5, the nitrogen oxides generation, principally monoxides and dioxides (NO and NO<sub>2</sub> respectively), are caused by the high temperature inside the cylinders, by favoring the oxidation of the molecular nitrogen.

On the other hand, in order to avoid the formation of soot, it is necessary to reduce the local fuel/air ratio ( $\phi$ ), to approximately a maximum of twice the stoichiometric value.

Thus, any strategy adopted with the objective of reduce the contamination must seek to avoid both regions of generation of pollutants.



One of the strategies to obtain a poor local mixture is by premixing the fuel with air before the start of combustion. This requires to extend the self-ignition delay time. One way to obtain this extension is acting on the properties of the gas introduced in the combustion chamber.

### **2.3.1 HCCI Engine**

The HCCI (Homogeneous Charge Compression Ignition) engine is an ideal engine model that, as its name indicates, works by exploiting a compression ignition of a homogeneous mixture of fuel and air, [5]. This model considers that the mixture simultaneously ignites in the whole volume of the cylinder, without a flame front.

This type of engine has an important challenges in order to be really useful for a mass production, barriers like the combustion phase control, due to the absence of a direct control to the ignition start; or the limited range of operation, influenced mainly by the fuel autoignition properties [2].

As a possible solution to these problems, a variant has been proposed, which can be considered the union of compression and spark ignition technologies.

### **2.3.2 SCCI Engine**

The Stratified Charge Compression Ignition engine is a modification of the HCCI idea, with the intention of solve these problems. It consists in the union of the two types of conventional engines. To properly operate, an external injection to the cylinder of a high resistance autoignition fuel (like in the SI engines) is combined with a direct injection of diesel or another fuel with low octane rating, which is responsible for initiating the combustion. For this reason it is also known as a mixed injection engine [10].

With the external injector the large part of the used fuel is preloaded in order to obtain a mixture as homogeneous as possible. In order to avoid an uncontrolled autoignition,

high octane fuels are used, such as gasoline, natural gas or liquid petroleum gas. The last two combustibles are used in this project.

As a result of the above, the mixture cannot ignite for itself, it is necessary therefore produce or introduce a detonator. In this case the detonator is a little part of diesel, injected near the Top Dead Center. It will ignite due to the high pressure and temperature conditions of the chamber, spreading the fire to the other fuel previously injected. Despite that, part of the homogeneity is lost, the local fuel/air ratio remains poor enough to avoid the soot formation region. Besides, the absence of a flame front causes that the temperature inside the engine to be low enough to reduce de formation of  $\text{NO}_x$ .

The air standard cycle that represents this type of combustion is the Sabathé cycle, the same as in the CI engines, shown in the section 2.2.3.

## 2.4 Fuel Injection System

The fuel injection is the process that replace the use of the carburetor in the reciprocating engines. In this process, the fuel is injected using electronically controlled injectors, that atomize the fuel inside the combustion chamber in the CI engines, in this or in the intake manifold in the SI engines, or both in the SCCI engines, [10].

### 2.4.1 Fuel injector for intake-manifold injection

The fuel gas (LPG or natural gas) is injected in the intake-manifold instead of inside the cylinder. The ECU calculates the amount of fuel required, at up of 450 kPa, and control the injectors, [12].

The electromagnetic fuel injectors, as the Figure 2.6, spray the fuel in the precise amount required.

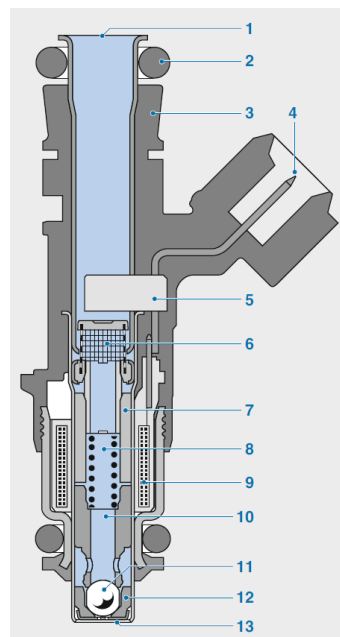


Figure 2.6: Intake Manifold Electromagnetic Fuel Injector, [12]

The injection operation is the following:

- When the injector isn't activated, the spring presses the needle and valve ball against the injection-orifice.
- At the moment that the injection is activated, the current that goes through the solenoid begin to rise, attracting the needle. In this moment, the fuel starts to be sprayed.
- When the needle reaches the top of the injector, the circulating current is maximum.
- The injection finishes after the dropout time has elapsed, when the current is turned off.

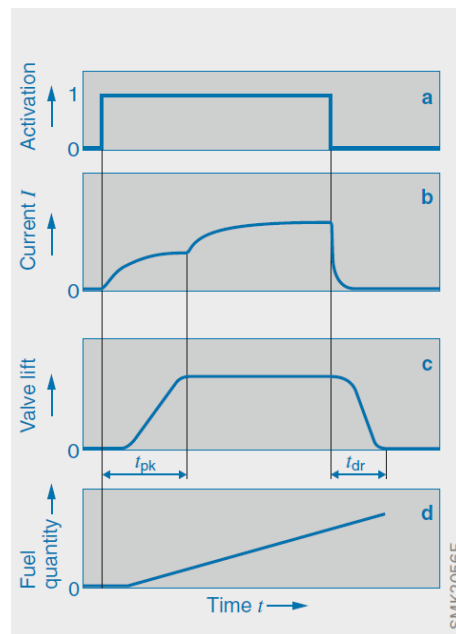


Figure 2.7: Injection-duration correction according to the battery voltage, [12]

The quantity of fuel injected is proportional to the time (Figure 2.7.d). The time elapsing between the activation signal and the start of the injection depends on the battery voltage. This time can be correct following the Figure 2.8.

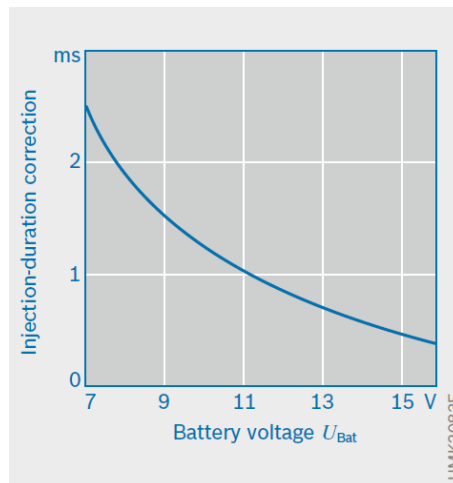


Figure 2.8: Injection-duration correction according to the battery voltage, [12]

### 2.4.2 Common-rail system

The common-rail system is a fuel injection system for the CI engines that generates the necessary fuel pressure for all injectors.

Through this system the fuel can be injected to the desired pressure, usually between 200 and 1.800 bar. It also allows to change the injection instant or to realize multiple injections per cycle too.

The main components can be classified into three groups:

- Low pressure: fuel supply system.
- High pressure: pump, common-rail and injectors.
- Electronic control: EDC, sensors and actuators.

The figure 2.9 shows the basic diagram of the common-rail systems. We can observe how the fuel increase its pressure in the high-pressure pump (Fig.2.9.1) before depositing it in the rail, who acts as buffer.

The pressure control is performed by the ECU. It compares the measured value by a sensor with the preset value. If the pressure is below that the desired, the pump is activated

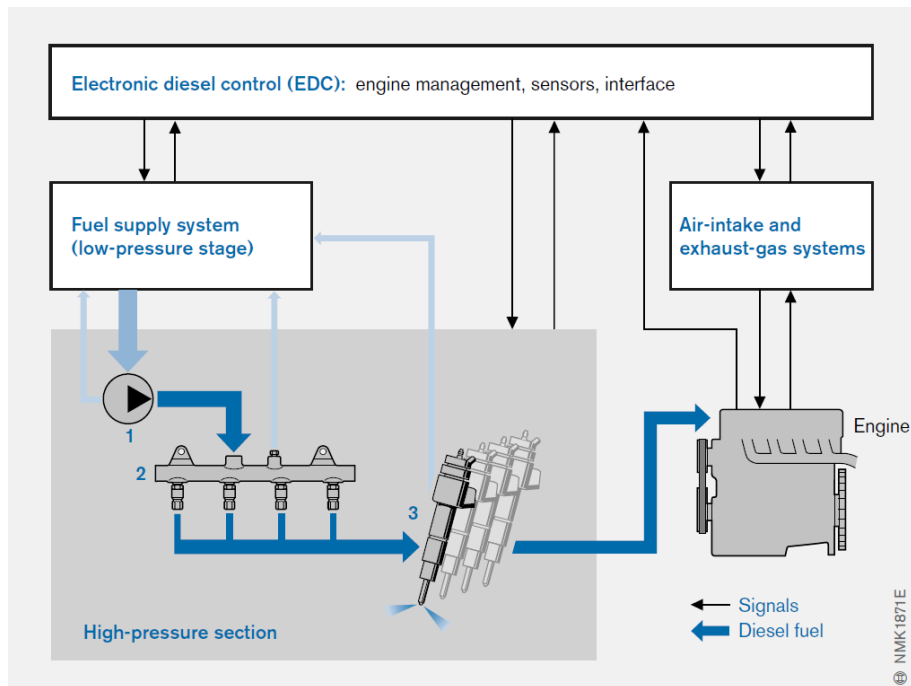


Figure 2.9: Diagram of the common-rail system, [11]

until it reaches it. If the pressure is above, the fuel returns to the tank through the pressure-relief valve, present in the rail. Thanks to this, the fuel pressure doesn't depend on either the amount of fuel injected or engine's speed.

### 2.4.2.1 Common-rail diesel injectors

In the common-rail systems the injectors, responsible to introduce the desired amount of fuel into the cylinders, are directly connected to the rail.

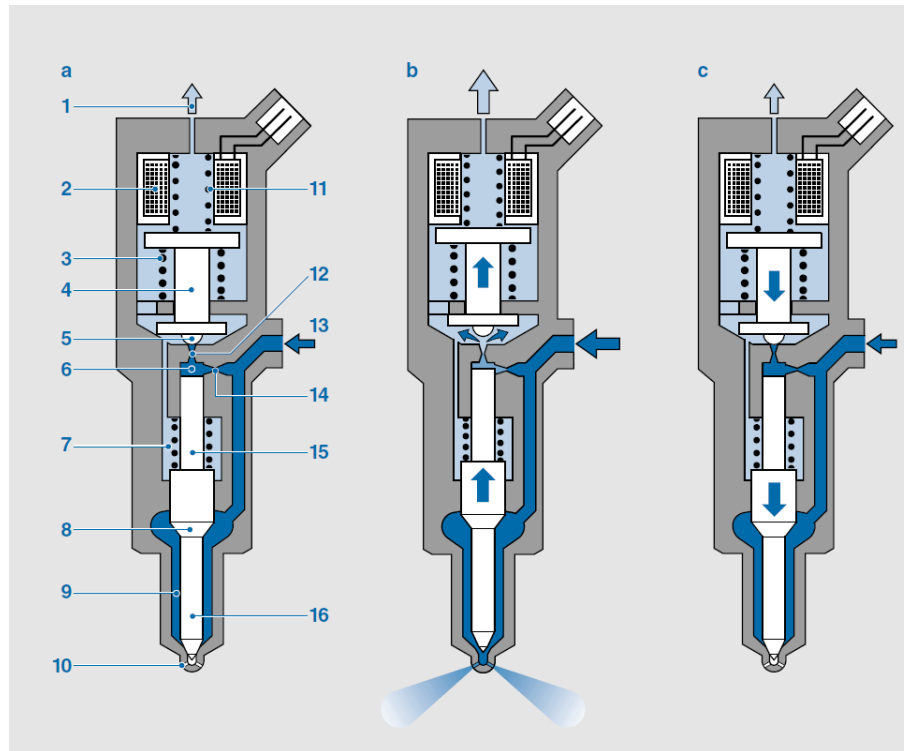


Figure 2.10: Diagram of the common-rail system, [11]

Their operation, illustrated in the Figure 2.10, is as follows:

- Injector closed (Fig.2.10.a): When the injector isn't activated, remains in the resting position, where the spring (11) press the ball on the outlet restrictor. The pressure on both sides of the needle is the same, therefore the spring (7) is able to keep the injector closed.
- Start of injection (Fig.2.10.b): In the moment that a high current starts to go through the solenoid (2) this, helped by the spring (3), attract the rod (4) and, with it, the ball that close the outlet restrictor. The pressure on the back of the needle decreases,

creating a difference that is able to overcome the spring resistance (7) and pushes upwards the needle, leaving the injector orifice open.

- c. End of injection (Fig.2.10.c): When the current is switched off, the solenoid releases the rod and the spring (11) pushes it. The outlet restrictor closes and, thus, the pressure on both sides be equated, allowing the spring (7) to stop the injector.



## 2.5 Engine Control Unit

The antipollution regulations of the different countries force the improvement of the efficiency of the engines, forcing to improve the control of the combustion processes. Because of this, the control of current internal combustion engines is carried out using electronic systems based on microcontrollers, replacing the previous electromechanical systems. In Figure 2.11 the basic control diagram is presented, including sensors, actuators and the engine control unit (ECU).

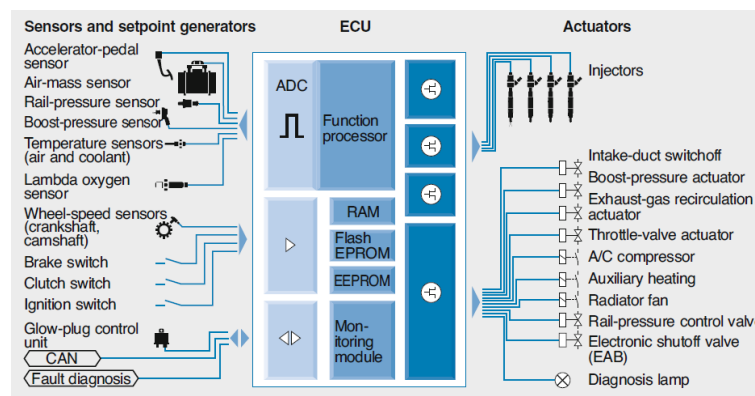


Figure 2.11: Main components of EDC, [11]

The sensors are the devices responsible for measuring the different variables of the operation of the engine, like injection pressure, position of accelerator pedal, the current of the injectors, among others.

On the other hand, the actuators are the devices responsible to carry out the work, such as fuel injectors or air and fuel pumps.

The ECU concentrates its digital intelligence in the microcontroller with its ADCs and the firmware, while the power stages and signal conditioners of the sensors allow the interaction with the engine.

The main systems controlled by the ECU are the gas circulation, the engine temperature and the injection system. This project is focused in this last system.



# **3 Specifications and Technologies required**

## **3.1 Introduction**

In this chapter, the required elements for the control of the dual fuel engine are exposed. Firstly, the characteristics of the engine used in this work, which in this case is a conventional diesel engine. This engine features an injection system, including the original diesel injectors and the added gas needed to perform the dual fuel mode.

Secondly, the instruments needed to create the digital intelligence are exposed. This tools are the STM32 NUCLEO-F401RE Development Board, in charge to control the whole system; the softwares STM32Cube and System Workbench for STM32, necessities to create the code; and the LabVIEW, as interface between the computer and the engine.

And finally, the Injection Control System is explained with the sequence to perform the diesel injection and the boost converter necessary to follow it.

## 3.2 KOHLER Diesel KDI 1903 TCR Engine

The engine used in this project is the model KDI 1903 TCR, manufactured by KOHLER. It is a three-cylinder engine of 42 kW (56 HP), turbocharged and with direct injection using a common-rail system.

### 3.2.1 Engine specifications

The main technical characteristics are reported in its user manual [7] and a summarized version is shown in the following table:

<b>Construction and operating specifications</b>	
Strokes	4
Cylinders	3
Bore	88 mm
Stroke	102 mm
Displacement	1861 cm <sup>3</sup>
Compression Ratio	17.4/1
Valves per cylinder	4
Injection	Direct – Common Rail
Dry Weight	233 kg
Cooling	Liquid

In the Fig. 3.1, we can see the performance curves of the KOHLER engine. The maximum torque (225 Nm) is located at 1500 rpm, while its maximum speed is 2600 rpm, with a power rating of 42 kW or 56 HP.

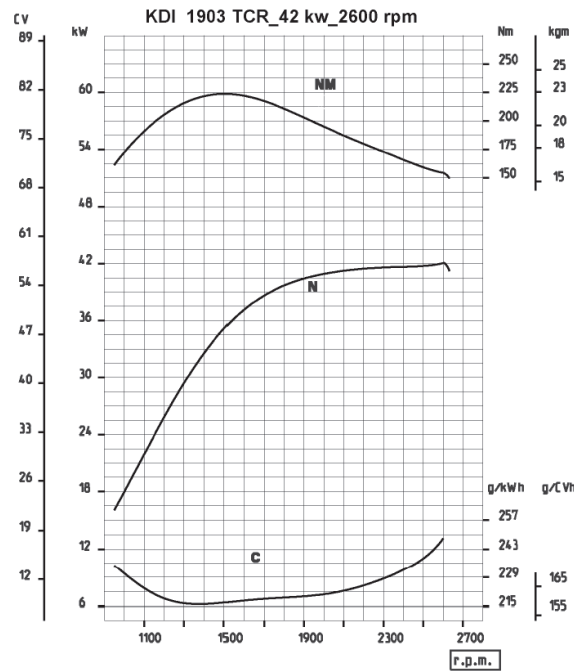


Figure 3.1: KDI 1903 TCR Performance Curves, [7]

### 3.2.2 Fuel Injection System

The original fuel injector system is formed by three diesel injectors joined to a variable pressure Common Rail, up to 2000 bar.

As it is a 4-stroke engine, the combustion in each cylinder is produced every two turns of the crankshaft ( $720^\circ$ ), then a combustion will occur every  $240^\circ$ . The trigger reference signal is given by square wave, that has the rising edge  $4^\circ$  before the TDC of the first cylinder, and the falling edge  $364^\circ$  before it.

In order to use the engine in a dual fuel fashion, we need to introduce a gas injector other than the diesel one and the resistance and inductance values of both types of injectors are shown in the following table:

Injector	Resistance ( $\Omega$ )	Inductance (mH)
Diesel injector	0.41	0.19
Gas injector	8.6	10.06

### 3.3 Digital intelligence

#### 3.3.1 STM32 NUCLEO-F401RE Development Board

The board used for the management of the engine injection system is the STM32 NUCLEO-F401RE development board (Fig. 3.2), manufactured by STMicroelectronics. It is based on the STM32F401RE 32-bit ARM microcontroller.

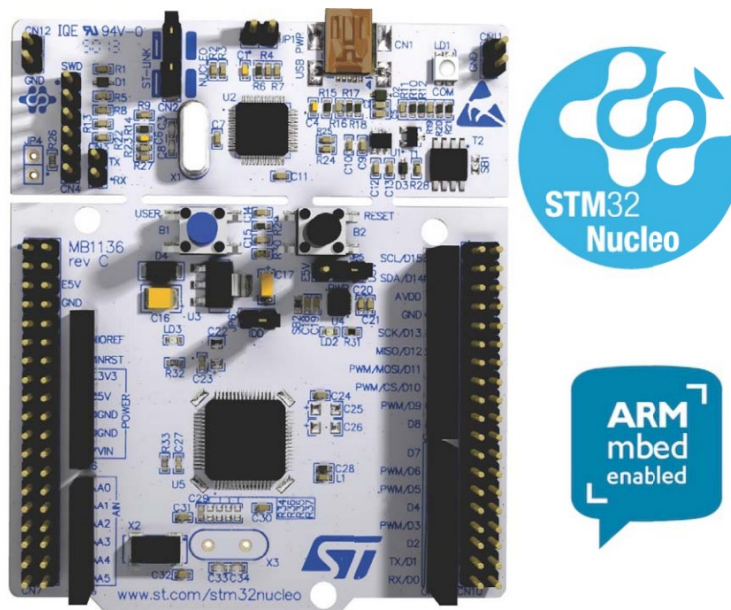


Figure 3.2: STM32 NUCLEO-F401RE development board, [18]

The STM32 Nucleo board provides high ease of expansion due to its compatibility with peripherals developed for the Arduino Uno V3 and the connectors ST Morpho. Also, its on-board ST-LINK/V2-1 debugger and programmer allows to link the board directly, via USB, to the host computer without additional hardware.

The main features of the NUCLEO-F401RE are the following:

- ARM 32-bit Cortex-M4 STM32F401RE microcontroller, with a frequency up to 84 MHz in LQFP64 package.
- Two types of expansion connectors:

- Arduino™ Uno V3.
- ST Morpho, with full access to all I/Os pins.
- On-board ST-LINK/V2 debugger and programmer.
- Possible supply voltages: 3.3 V, 5 V or 7-12 V.
- Three LEDs:
  - LD1: USB Communication.
  - LD2: Programmable.
  - LD3: Supply.
- One reset button and one programmable.

The STM32F401RE microcontroller, present in the STM32 Nucleo board, is part of the STM32F401xD/xE microcontrollers family. They are devices based on 32-bit ARM Cortex-M4 core and RISC architecture. This family operates at a frequency up to 84 MHz and the Instruction set also performs DSP instructions, which allow to achieve mathematical operations at very high speed.

Some of the main features of the STM32F401RE microcontroller are the following:

- 32-bit ARM Cortex-M4
- 1.25 DMIPS/MHz (millions of instructions per second at 1 MHz, according to Dhrystone 2.1 benchmark).
- DSP instructions.
- Frequency up to 84 MHz.
- Memories:
  - 512 Kbytes of flash memory.
  - 96 Kbytes of SRAM memory.
- 16-channel 12-bit resolution ADC at 2.4 MSPS (millions of samples per second).
- 11 general-purpose timers.
- 12 communication interfaces:
  - 3 I<sup>2</sup>C

- 3 USARTs
- 4 SPIs
- 1 USB 2.0
- 81 GPIO ports with interrupt capability, 78 of them with a maximum frequency of 42 MHz. All of them are 5 V tolerant.

These characteristics are summarized in Fig. 3.3 and, in Fig. 3.4, the existing peripherals being clearly visible in the block diagram.

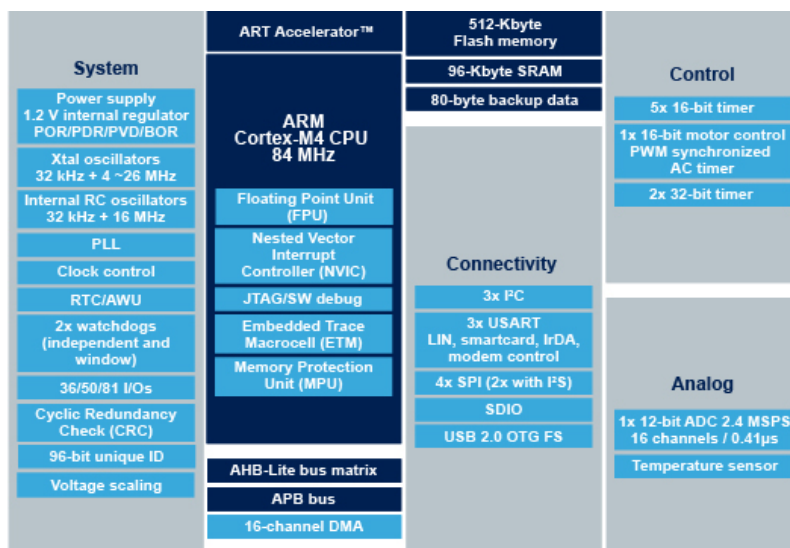


Figure 3.3: Summary of the main features of the STM32F401xD/xE microcontrollers, [13]

### 3.3.1.1 General-purpose I/Os (GPIOs)

The general-purpose input/outputs of the STM32F4 microcontrollers provide an interface between the CPU and the environment. They provide a bidirectional channel. Each GPIO can be independently configured as output (push-pull or open-drain) or input, both with or without pull-up or pull-down resistors.

Most of the 81 GPIO pins are shared with some other peripherals, whether for analog or digital functions.



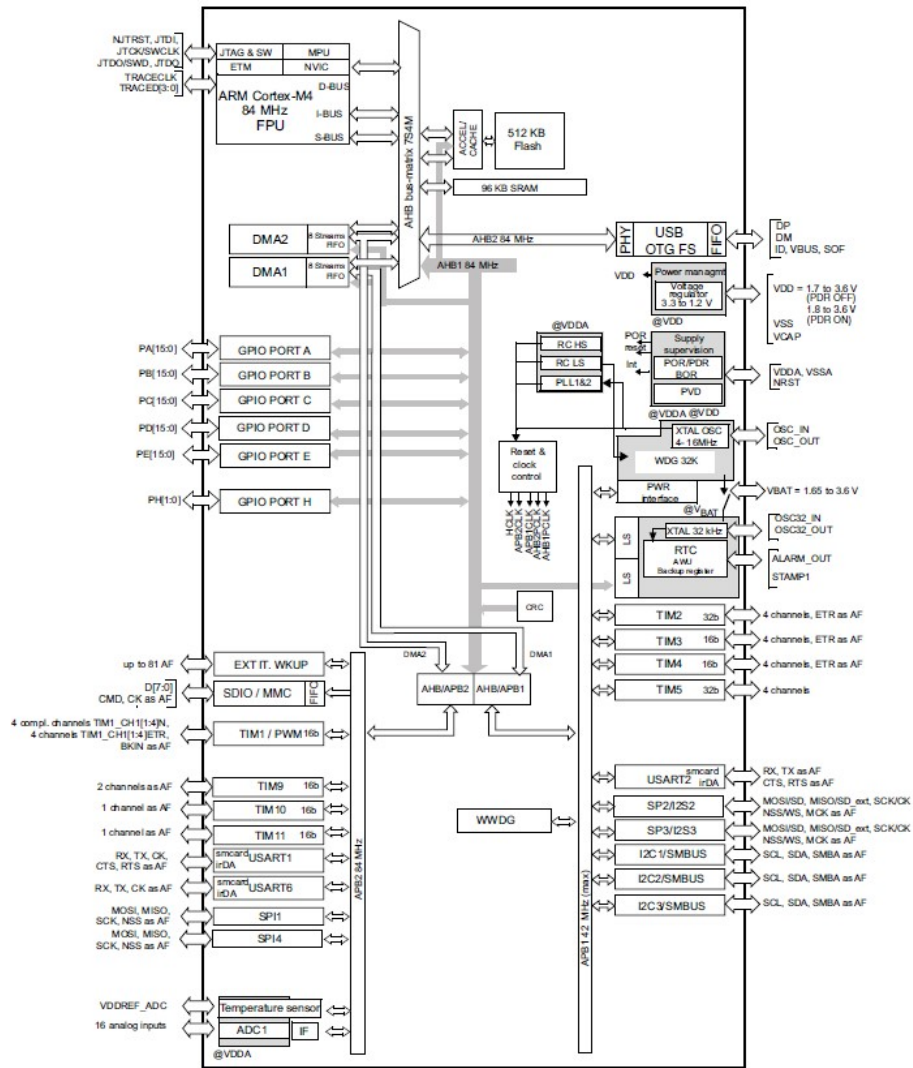


Figure 3.4: Block diagram of the STM32F401xD/xE microcontrollers, [16]

The I/Os are grouped into five 16-pin ports, named in alphabetical order, from GPIOA to GPIOE, plus a single pin named GPIOH. All these ports, as shown in Fig. 3.4, are directly connected to the AHB1 bus, allowing operate each pin at a frequency of up to 84 MHz.

### 3.3.1.2 Timers and counters

The STM32F401xD/xE microcontrollers are equipped with 11 timer/counters, 10 general-purpose (TIM2-6, 9-11) and one advance-control (TIM1). Their main characteristics are reported in Fig. 3.5.

Timer type	Timer	Counter resolution	Counter type	Prescaler factor	DMA request generation	Capture/compare channels	Complementary output	Max. interface clock (MHz)	Max. timer clock (MHz)
Advanced-control	TIM1	16-bit	Up, Down, Up/down	Any integer between 1 and 65536	Yes	4	Yes	84	84
General purpose	TIM2, TIM5	32-bit	Up, Down, Up/down	Any integer between 1 and 65536	Yes	4	No	42	84
	TIM3, TIM4	16-bit	Up, Down, Up/down	Any integer between 1 and 65536	Yes	4	No	42	84
	TIM9	16-bit	Up	Any integer between 1 and 65536	No	2	No	84	84
	TIM10, TIM11	16-bit	Up	Any integer between 1 and 65536	No	1	No	84	84

Figure 3.5: Features of STM32F401RE timers, [16]

The timers are a series of peripherals formed by synchronous circuits. Their functions consist on counting of pulses. Depending on the origin of these pulses we can find two types of peripherals: timers if the origin of pulses is an oscillator at constant frequency; or counter if the pulse source is another external signal.

In the microcontroller, its peripheral timers can be classified into two groups according to some of its functionalities:

- General-purpose timers (TIM2-5,9-11): The general-purpose timers are used in a large number of applications where it is necessary to count the time between two events, generate a delay or obtain the frequency of a signal external pulses. There are seven general-purpose timers in the STM32F401xD/xE microcontrollers. Four

of them, TIM2-5, are equipped with four independent channels, while the TIM9 has two, and the TIM10 and 11 only one each one. The resolution of the counters and their counting mode can be observed in Figure 3.5, with the following modes of operation, [17]:

- Input capture mode: Obtain the frequency from an external signal.
- Output compare mode: It is used to generate a pulse signal or to indicate when a preset time period has elapsed.
- PWM mode: Mode to generate a PWM signal.
- One pulse mode: It is a combination of the first two modes, generating a pulse with a certain delay as a response to a stimulus.

Timers TIM2-5 can work independently or together, while TIM9-11 can be synchronized to them, or simply be used as a time base.

- Advanced-control timer (TIM1): This timer differs from the previous ones by its ability to generate three complementary PWM, with a programmable dead time between them. It can also work jointly with the others timers.

### 3.3.1.3 ST-LINK/V2 debugger and programmer

The ST-LINK/V2 circuit is a debug/programmer circuit present in the NUCLEO-F401RE used in this project. This circuit communicates with the microcontroller through the SWD (Serial Wire Debugging) interface.

Communication with the PC is via the high-speed USB interface.

### 3.3.1.4 Analog-to-digital converter

An analog-to-digital converter is a peripheral present in most microcontrollers. Its function is to convert an analog input signal, such as the output of a sensor, into a digital signal. The STM32F401xD/xE microcontrollers are equipped with a 12-bit A/D converter, multiplexed into 16 channels.

Its operating modes are as follows, [15]:

- Single-channel, single conversion mode: It is the simplest mode of operation. It performs one measurement only and it ends after conversion.
- Multichannel (scan), single conversion mode: This mode is used to measure several channels sequentially. Each one can have different sampling times.
- Single-channel continuous conversion mode: This mode samples a single channel continuously in the background, without any intervention from the CPU.
- Multichannel (scan) continuous conversion mode: This mode differs from the previous multichannel in that when the sample of the last channel ends, the peripheral does not stop, but starts again with the first one.
- Injected conversion mode: This mode has priority over all previous ones. When the peripherals receives a pulse by software or by an external event, it interrupts any current measure to carry out a higher priority conversion. When it ends, the interrupted measure resumes.

### **Analog-to-digital converter features**

The electrical and time characteristics in the general operating conditions are described hereafter.

With a supply voltage between 2.4 and 3.6 V, the converter frequency clock can span between 0.6 and 36 MHz, being 30 MHz the typical frequency. The frequency used for the peripheral is the maximum.

The sampling time is obtained by the following equation:

$$t_S = \frac{n^\circ \text{ of samples}}{f_{ADC}} \quad (3.1)$$

Being 3 the minimal number of samples and 480 the maximum, the sampling time is between 83.3 ns and 13.3  $\mu$ s.

The conversion time is calculated by the following equation:

$$t_{conv} = \frac{\text{resolution bits}}{f_{ADC}} \quad (3.2)$$

Thus, the conversion time to 36 MHz is between 166.67 and 333.33 ns, for 6 and 12 bits respectively.

The time interval necessary to obtain a measure, with a sampling time of 3 cycles at 36 MHz and 12 bits of resolution, is 0.25  $\mu\text{s}$ .

The following table shows in detail the time to 30 MHz for different resolutions:

Symbol	Parameter	Conditions	Min	Typ	Max	Unit
$t_{lat}^{(2)}$	Injection trigger conversion latency	$f_{ADC} = 30 \text{ MHz}$	-	-	0.100	$\mu\text{s}$
			-	-	$3^{(5)}$	$1/f_{ADC}$
$t_{lat}^{(2)}$	Regular trigger conversion latency	$f_{ADC} = 30 \text{ MHz}$	-	-	0.067	$\mu\text{s}$
			-	-	$2^{(5)}$	$1/f_{ADC}$
$t_S^{(2)}$	Sampling time	$f_{ADC} = 30 \text{ MHz}$	0.100	-	16	$\mu\text{s}$
			3	-	480	$1/f_{ADC}$
$t_{STAB}^{(2)}$	Power-up time		-	2	3	$\mu\text{s}$
$t_{CONV}^{(2)}$	Total conversion time (including sampling time)	$f_{ADC} = 30 \text{ MHz}$ 12-bit resolution	0.50	-	16.40	$\mu\text{s}$
		$f_{ADC} = 30 \text{ MHz}$ 10-bit resolution	0.43	-	16.34	$\mu\text{s}$
		$f_{ADC} = 30 \text{ MHz}$ 8-bit resolution	0.37	-	16.27	$\mu\text{s}$
		$f_{ADC} = 30 \text{ MHz}$ 6-bit resolution	0.30	-	16.20	$\mu\text{s}$
		9 to 492 ( $t_S$ for sampling +n-bit resolution for successive approximation)				

Figure 3.6: Characteristic times of the ADC converter.

### 3.3.2 STM32Cube

STM32Cube is a platform created by STMicroelectronics with the aim of facilitating the code development for the microcontrollers of the same company.

It consists of two parts: the STM32CubeMX initialization code generation and a set of supporting libraries.

The STM32CubeMX software is a tool that allows to generate the initialization code using a Graphic User Interface assistant. The process needed to generate the project can be seen in Figure 3.7.

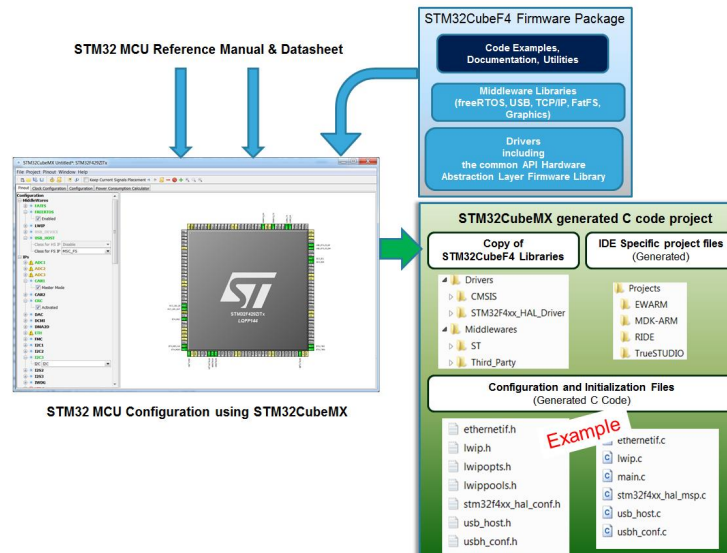


Figure 3.7: Overview of STM32CubeMX C code generation flow, [20]

The main characteristics are as follows, [20]:

- Project management. The STM32CubeMX allows to create and modify them. It also allows importing previously projects to create new ones.
- Easy microcontroller and board selection using a tailored wizard.
- Selection of peripherals using the visual interface or from drop down list, both visible in the main window, shown in Figure 3.8.
- Generation of the project, with all the necessary libraries and source files. It also allows to execute changes in these files, adding or removing information of certain sections dedicated in the code.
- It allows to visualize and modify the configuration of the microcontroller's clocks and each peripheral, allowing to avoid possible conflicts.

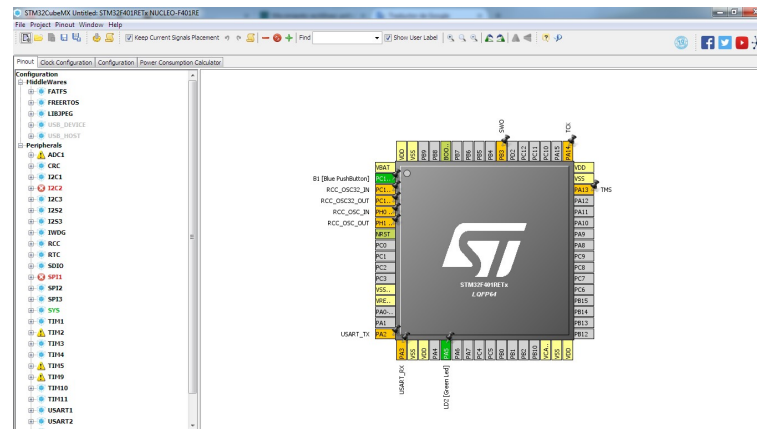


Figure 3.8: STM32CubeMX main window

This software also includes a set of support libraries, which are STMCube HAL and Low-Layer (LL) APIs, [19]

The STMCube HAL is an abstraction layer, composed of a set of APIs (Application Programming Interface). Its purpose is to help create applications without to need to know in depth the microcontroller used, also allowing the portability among different microcontrollers of STM32 family [21].

They are divided in two categories: generic APIs, with the common functions for all STM32 microcontrollers; and extension APIs, with specific functions for each family.

The Low-Layer API is closer to the hardware than the HAL. Therefore, it is lighter and better optimized, both performance and runtime.

Both APIs can work together, taking into account some restrictions.

### 3.3.3 System Workbench for STM32 (SW4STM32)

Programming of the STM32 board has been done using the System Workbench for STM32 tool. This Integrated Development Environment (IDE) is provided by AC6 (Assistance Conseil Systèmes) and supports most of the STM32 microcontrollers.

The main characteristics are as follows, [14]:

- Support for STM32 devices, whether microcontrollers or development boards.
- C/C++ compiler based on GCC.
- GCB based debugger.
- ST-Link/V2 support.
- No code size limitation.

### 3.3.4 System development environment NI LabVIEW

LabVIEW, acronym of Laboratory Virtual Instrument Engineering, is a development environment for a visual programming language, developed by National Instruments. This environment has simplified the application programming by replacing the typical programming languages by graphical objects and functions.

Since the software was initially focused on the realization of electronic instrumentation control applications, each application created with this software is called as VI or Virtual Instrument. Currently, the software functions have been extended beyond the control of electronic equipment and is also used in areas such as communications, embedded programming or automation systems.

#### 3.3.4.1 Execution structures

The execution structures allow the control of the code located inside. The structures used in the project are described below.

- While Loop: The While Loop cycle has the function to repeat the code inside until a specific condition occurs. It has an Iteration Terminal, that provides the number of completed iterations, which will be one at least. It also performs a Conditional Terminal, which can stop the loop if some predetermined boolean values or error signals are met.





Figure 3.9: While Loop

- **Case Structure:** This structure has the function of executing one of the internal sub-diagrams, similarly to the if-else or switch statements in the classical programming languages. The selection condition can be an integer or boolean value, or a string.

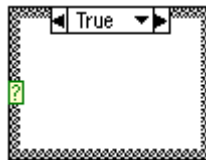


Figure 3.10: Case Structure

#### 3.3.4.2 VISA Functions

The VISA functions are preprogrammed VIs and functions that facilitate the control of instruments or the use of a standard interface, such as GPIO, USB or serial, among others.

The main functions used in the project are described bellow.

- **VISA Configure Serial Port:** This function is responsible to initialize the serial port specified by VISA resource name identifier. In particular it the type of termination char, baud rate, parity or stop bits, among others, are specified.
- **VISA Write:** The function of this object is to send data from the instrument to the opened communication channel.
- **VISA Read:** Its function is to collect the information transmitted by the instrument stored in a designed memory buffer.

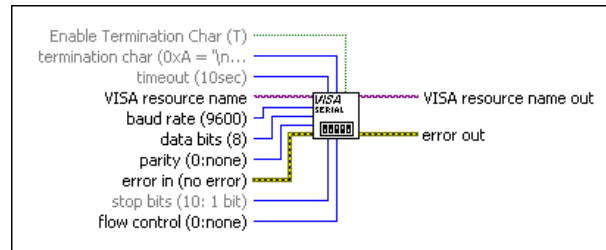


Figure 3.11: VISA Configure Serial Port Diagram

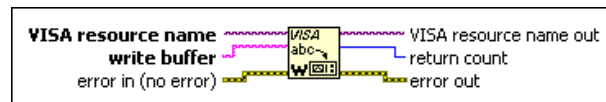


Figure 3.12: VISA Write Function Diagram

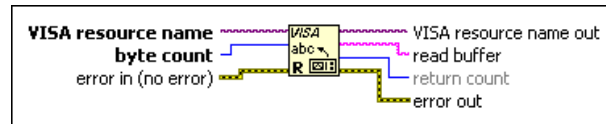


Figure 3.13: VISA Read Function Diagram

- VISA Close: Using this object, we can close the communication channel with the instrument.

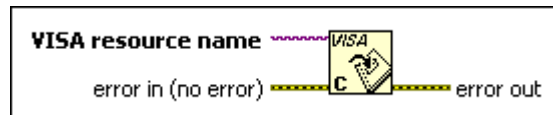


Figure 3.14: VISA Close Function Diagram

## 3.4 Injection system control

### 3.4.1 Control sequence of diesel injectors

The fuel injectors, as explained in the Section 2.4.2, are the electromagnetic devices responsible to introduce the necessary amount of fuel into the combustion chambers.

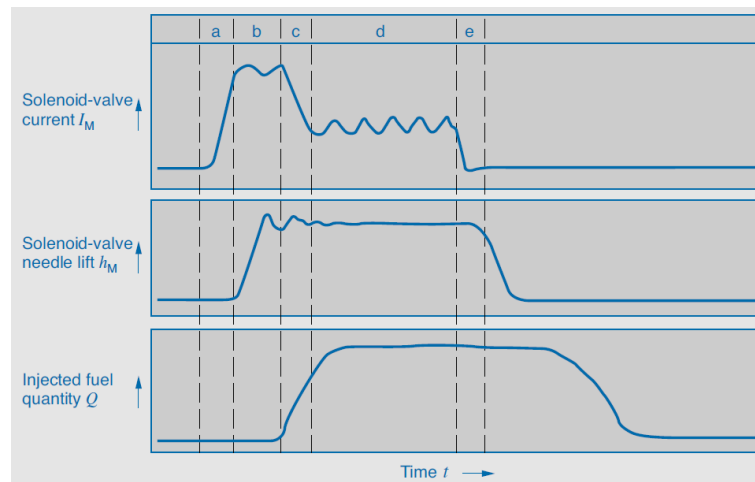


Figure 3.15: Diesel fuel injection sequence, [11]

The aperture control process of the injectors, as shown in Figure 3.15, is as follows:

- a. Opening phase: The first step in the fuel injection consists in a quick injector opening. With the objective to reach a high levels of reproducibility, the aperture is performed by a high current flank, up to 20 A, significantly higher than its nominal value. In order to obtain a rapid rise of the current, it is necessary to use a boost converter, that provides 50 V (calculated in the section 3.4.2), starting from the available 12 V of a standard engine battery.
- b. Pickup-current phase (optional): Once the maximum current is reached, this is maintained by exchanging the boost with the battery. Even if this stage has been taken into consideration, it wasn't used in the current project.

- c. Transition to holding current phase: With the injector fully open, the required maintenance current is a lower value, around 9 A in our case. The excess energy from the solenoid is driven to the boost capacitor.
- d. Holding-current phase: The holding-current is supplied by the battery, by using a current control at 9 A.
- e. Switch-off: The injector is disconnected from the battery, forcing the accumulated energy going towards the boost converter. Due to its mechanical nature, and therefore being significantly slower than electronics driving, the injector takes several microseconds to stop the fuel injection.
- f. Recharging of the capacitor of the boost converter: Due to the process described, the converter has lost some of its charge. Therefore, the time between injections is used to recharge it to the desired voltage.

### 3.4.2 Boost converter Voltage

As discussed in the previous section, to obtain a rapid increase of the current, it is necessary to use a step-up converter. To obtain a correct response, the inductance must be able to reach the maximum current in around  $100 \mu\text{s}$  [4].

Using the following equation the current response curves of the injector solenoid are obtained:

$$i = \frac{V}{R} \cdot (1 - e^{-Rt/L}) \quad (3.3)$$

By using this simple equation and the typical electric values of the diesel injector ( $0.41 \Omega$  of resistance and  $0.19 \text{ mH}$  of inductance), Figure 3.16 shows the obtained charging times.

In the paper [4] the use of  $70 \text{ V}$  was recommended but, as we can see in the Figure 3.16, it is enough a  $50 \text{ V}$  value, as recommended by Bosch [11], to obtain a good response.

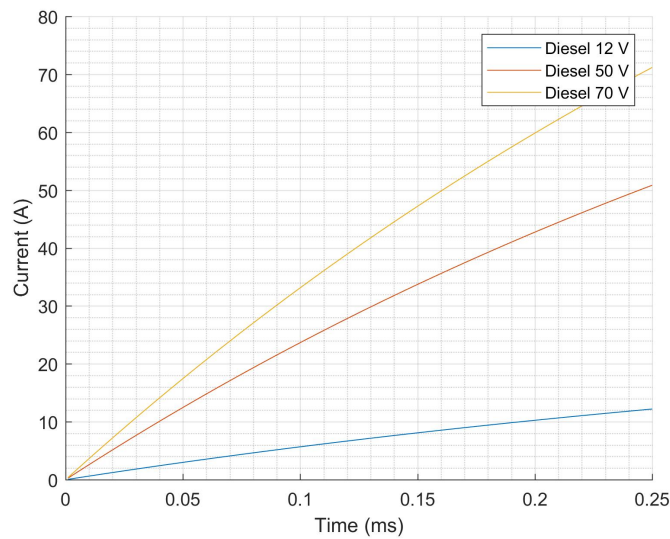


Figure 3.16: Injector currents at different voltages

### 3.4.3 Boost Converter

The DC-to-DC converters are power circuits dedicated to convert a DC voltage levels in other different values.

The most used type of regulator is the switching converter. This type of converter usually has a main transistor that functions as a switch, activating or deactivating it completely (saturation and cutoff in MOSFET transistors). They are very efficient devices, being widely used in power applications.

The topology used is the step-up or boost converter. They can obtain an output voltage higher than the input one.

The basic diagram of the boost circuit is shown in Figure 3.17. As a switch, a MOSFET or IGBT transistor is normally used.

The boost converter operates in two different states, closed switch and open switch.

When the switch is closed (Figure 3.18), the diode is inversely polarized. This makes the voltage between the inductance terminals is equal to the input voltage minus the transistor voltage drop in conduction ( $V_{in} - V_{DS(ON)}$ ), then causing the growth of the charge

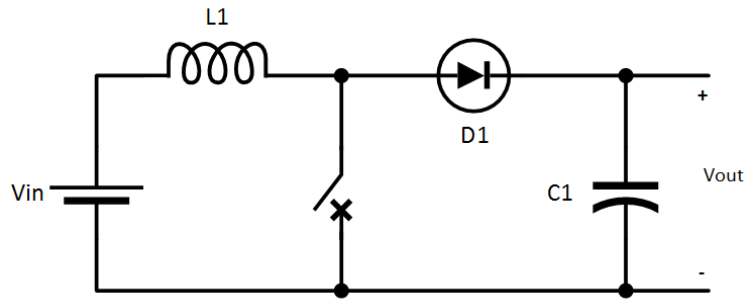


Figure 3.17: Boost Converter diagram

in the inductor. If the load is connected, it is fed by the capacitor.

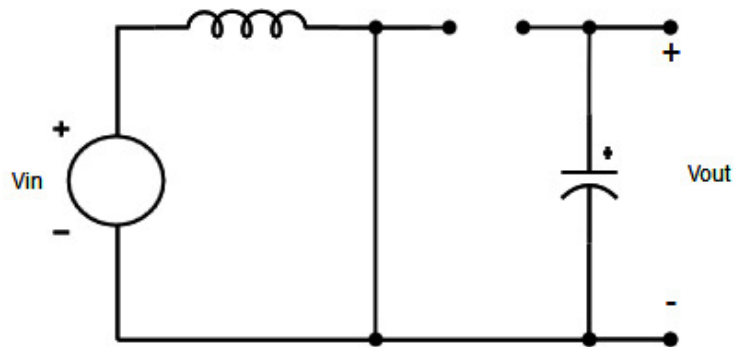


Figure 3.18: Equivalent circuit with the switch closed (MOSFET ON)

When the switch is opened instead, (Figure 3.19), the diode starts to conduct the current from the power supply to the load. During this stage, both the source and the inductance transfer energy to the load and to the capacitor.

In the steady state, considering that the converted is formed by ideal components, the average voltage is zero, satisfying the following equation:

$$V_{in} \cdot D \cdot T + (V_{in} - V_{out}) \cdot (1 - D) \cdot T = 0 \quad (3.4)$$

Clearing the voltages the transfer function of the converter is obtained:

$$\frac{V_{out}}{V_{in}} = \frac{1}{1 - D} \quad (3.5)$$

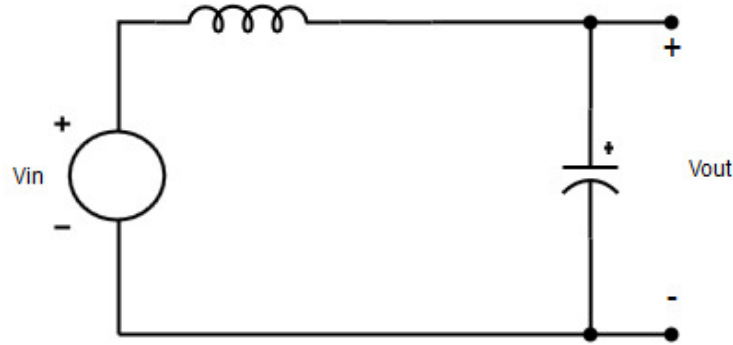


Figure 3.19: Equivalent circuit with the switch open (MOSFET OFF)

Where  $D$  is the duty cycle of the ON state of the transistor. But in a converter with real components the equation is more complex and it appears as follows:

$$(V_{in} - V_{DS(ON)} - r_L \cdot I_{in}) \cdot D \cdot T = (V_{out} + V_F + r_L \cdot I_{in} - V_{in}) \cdot (1 - D) \cdot T \quad (3.6)$$

Being  $V_F$  the direct voltage drop,  $r_L$  the inductor resistance and  $R$  the load resistance, clearing the input voltages the following transfer function is obtained:

$$\frac{V_{out}}{V_{in}} = \frac{1 - \left( \frac{V_{DS(ON)} \cdot D}{V_{in}} + \frac{V_F \cdot (1 - D)}{V_{in}} \right)}{(1 - D) \cdot \left( 1 + \frac{r_L}{(1 - D)^2 \cdot R} \right)} \quad (3.7)$$

Since  $V_{DS(ON)}$  and  $V_F$  values are very small with respect to the input voltage, they can be neglected, thus leaving the resulting transfer function:

$$\frac{V_{out}}{V_{in}} = \frac{1}{(1 - D) \cdot \left( 1 + \frac{r_L}{(1 - D)^2 \cdot R} \right)} \quad (3.8)$$





# 4 Experimental results

## 4.1 Introduction

This last chapter describes the designed Power Stage, the virtual instrument created with the LabVIEW software, the code implemented and executed within the microcontroller and the results obtained so far.

## 4.2 Power Stage Design

The Engine Control Unit, as defined in the section 2.5, is the device responsible to control the operation of an engine.

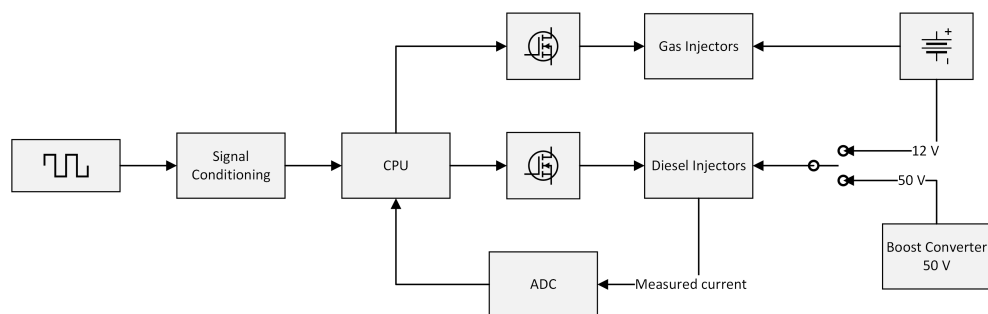


Figure 4.1: Conceptual diagram of the injector system

The conceptual diagram of the injector system can be seen in Figure 4.1. We can observe the ECU, with two input signals (crankshaft position and the current of the diesel

injectors) and the control signals of both types of injectors.

### 4.2.1 General Electrical Schematic of the injection system

Figure 4.2 shows the general electrical schematic of the power stages of both type of injectors.

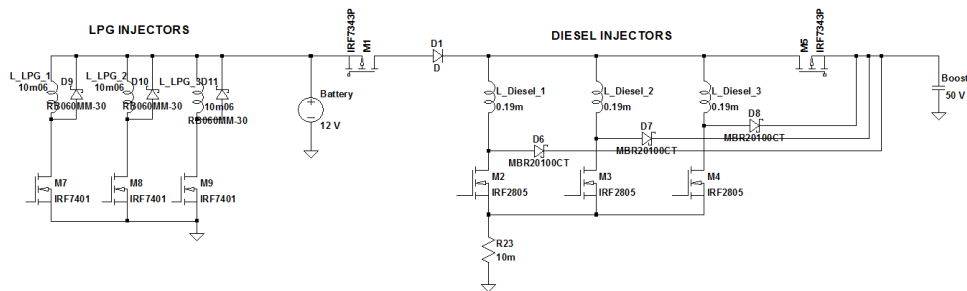


Figure 4.2: General Electrical Schematic of the injection system

### 4.2.2 Diagram of the gas injection system

Figure 4.3 shows the electrical schematic of the gas injectors. The selection of the injectors is performed by the MOSFET transistor located on the low side. In these injectors, the addition of the fuel starts as soon as the transistor closes. When the transistor is opened, the inductance is discharged through the flyback diode. The MOSFET driver is explained in section 4.2.4.

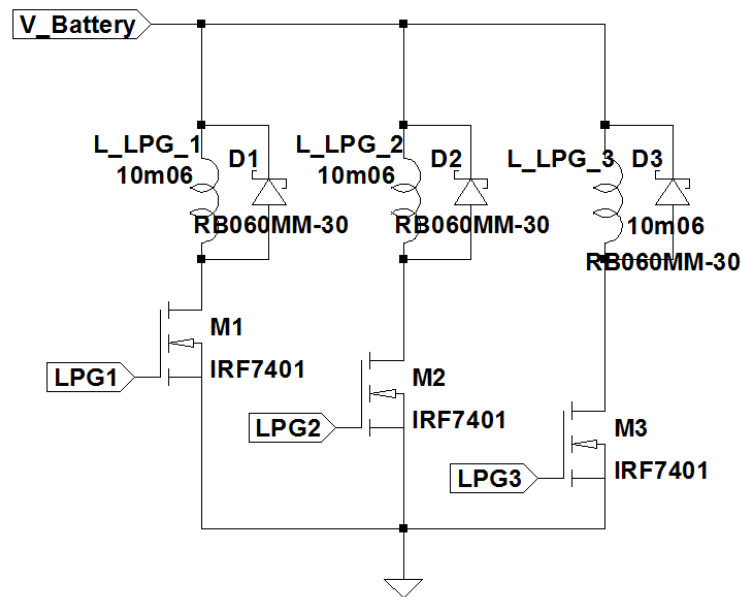


Figure 4.3: Gas Injection Schematic

### 4.2.3 Diesel injection system

The schematic of the diesel injection system, shown in Figure 4.4, is a bit more complex than the gas injection system. This is because this system needs to work at two different voltages levels, as explained in Section 3.4.2.

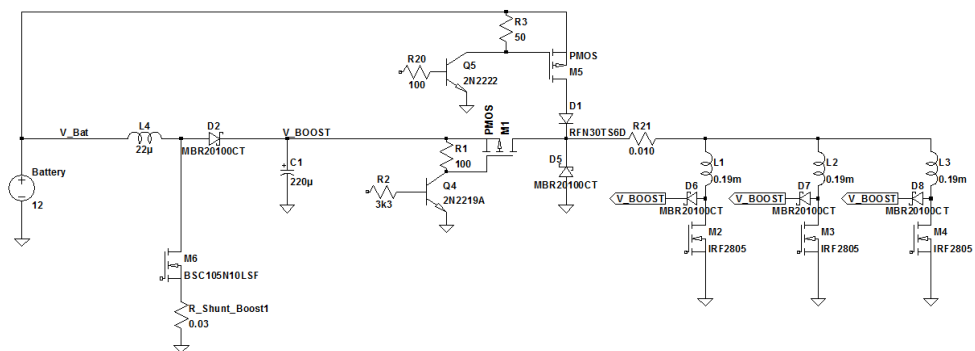


Figure 4.4: Diesel Injection Schematic

### 4.2.3.1 Control design of the Boost Converter

The 50 V power supply is provided by a boost converter (Section 3.4.3).

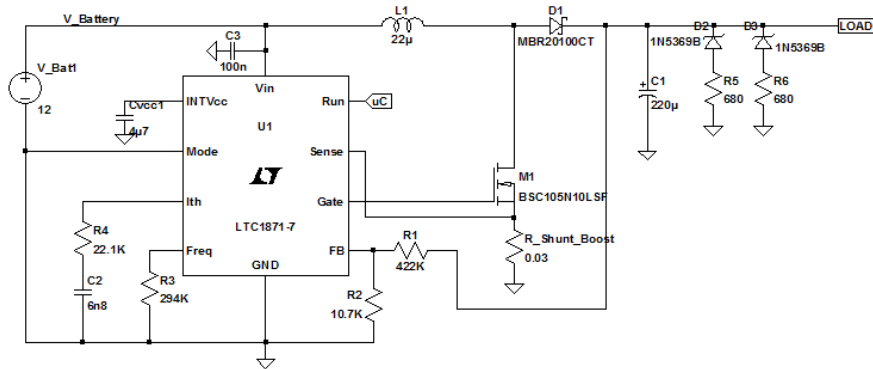
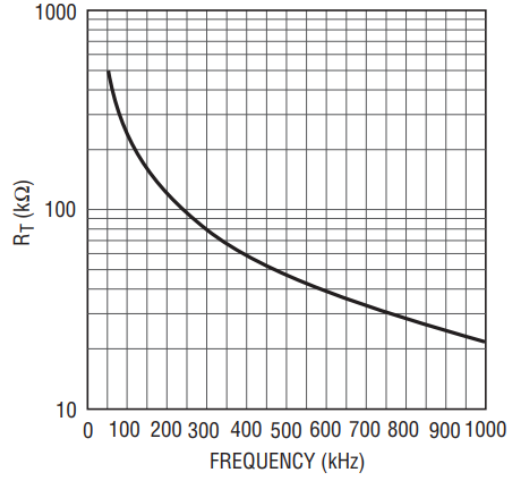


Figure 4.5: Boost Converter Circuit

The step-up converter has been designed to charge the capacitor that usually works to eliminate the ripple. In this case, this capacitor is responsible of the energy transfer toward the load, when it is connected by means of a MOSFET transistor.

To control the converter, the LTC1871-7 component, manufactured by Linear Technology, has been chosen. The design of the elevator converter has been performed by the following calculations:

The chosen operation frequency is 100 kHz, which allows to choose a relatively small sizes inductance. For this reason and according to Figure 4.6, a 294 k $\Omega$  resistance was placed between Freq pin and ground.

Figure 4.6: Timing Resistor ( $R_T$ ) Value, [8]

The desired output voltage was chosen by a voltage divider between the output voltage and the FB pin. The resistance values are calculated by the following equation:

$$V_o = 1.23 \cdot \left(1 + \frac{R_2}{R_1}\right) \rightarrow \frac{R_2}{R_1} = \frac{50}{1.23} - 1 = 39.65 \quad (4.1)$$

By choosing  $6.8 \text{ k}\Omega$  as  $R_1$  and  $270 \text{ k}\Omega$  as  $R_2$  the following voltage was obtained:

$$V_o = 1.23 \cdot \left(1 + \frac{270k}{6k8}\right) = 50.07 \text{ V} \cong 50 \text{ V} \quad (4.2)$$

The maximum attainable duty cycle is calculated by the following equation:

$$D = \frac{V_o + V_D - V_{IN(min)}}{V_o + V_D} = \frac{50 + 0.85 - 10}{50 + 0.85} = 80.33 \% \quad (4.3)$$

The resistor used to sense the current is calculated as follows:

$$R_{sense} \leq V_{sense(max)} \cdot \frac{1 - D_{max}}{\left(1 + \frac{\chi}{2}\right) \cdot I_{o(max)}} \quad (4.4)$$

$$R_{sense} = 0.8 \cdot 0.115 \cdot \frac{1 - 0.8033}{\left(1 + \frac{0.4}{2}\right) \cdot 0.5} = 0.0302 \cong 30 \text{ m}\Omega \quad (4.5)$$

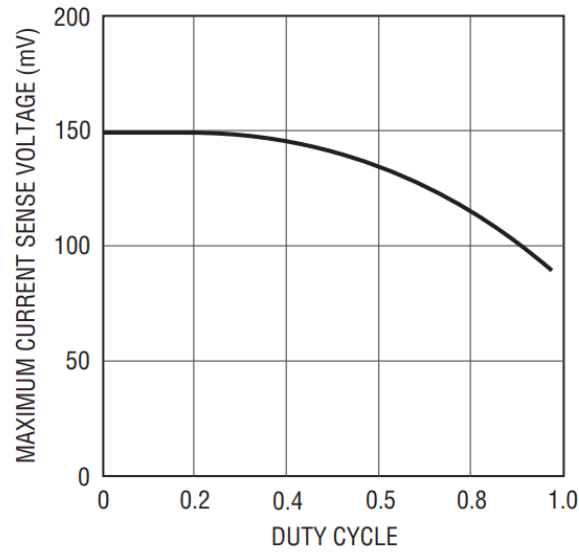


Figure 4.7: Maximum SENSE Threshold Voltage vs Duty Cycle, [8]

So a  $30\text{ m}\Omega$ . resistance was chosen.

#### 4.2.3.2 Supply voltage selection

##### Boost converter selection (50 V)

As a switch to connect the 50 V from the boost converter to the injectors it has been decided to employ the P-Channel MOSFET transistor IRFP9140N. This MOSFET, together BJT 2N2218 that drive it, is shown in the Figure 4.8.

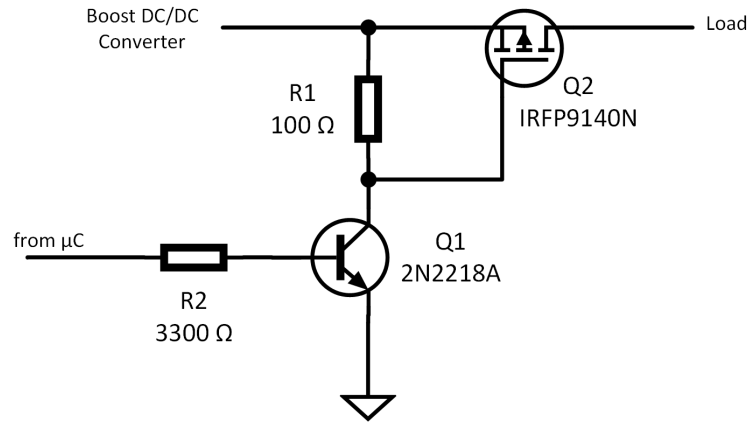


Figure 4.8: High Side Mosfet Driver

The voltage difference between gate and source of the MOSFET must be a maximum of 20 V, thus preventing the complete switching of the BJT. Therefore, the BJT must work in the active region, without going into saturation.

A voltage difference of 10 V between source and gate was chosen. Placing a resistance of  $100\ \Omega$  between both terminals, the current going through the resistor and therefore entering in the BJT's collector is:

$$I_R = I_C = \frac{-(-V_{GS})}{R_{GS}} = \frac{10\ V}{100\ \Omega} = 0.1\ A = 100\ mA \quad (4.6)$$

Considering a gain  $h_{FE}$  ( $\beta$ ) of 100, the current at the base of the BJT is:

$$I_B = \frac{I_C}{\beta} = \frac{100\ mA}{100} = 1\ mA \quad (4.7)$$

Since the input voltage from the microcontroller is 3.3 V, the resistance placed between the I/O driving pin and the base of transistor is:

$$R_B = \frac{V_{BB}}{I_B} = \frac{3.3\ V}{1\ mA} = 3.3\ k\Omega \quad (4.8)$$

With a collector current of 100 mA and a voltage drop between collector and emitter of 40 V, the losses in the BJT 2N2218N are:

$$P_{T(max)} = V_{BE} \cdot I_B + V_{CE} \cdot I_C = 0.7 \text{ V} \cdot 1 \text{ mA} + 40 \text{ V} \cdot 100 \text{ mA} \cong 4 \text{ W} \quad (4.9)$$

The maximum time that the transistor is used in each injection is  $200 \mu\text{s}$ . If we use it three times per engine cycle, even at maximum rotation regime (2600 rpm), the minimum period is 46.2 ms and the average dissipated power is:

$$P_{T(med)} = P_{T(max)} \cdot \frac{3 \cdot t_{inj(max)}}{T_{cycle}} = 4 \cdot \frac{3 \cdot 200 \mu\text{s}}{46.2 \text{ ms}} = 0.052 \text{ W} \quad (4.10)$$

As the transistor can dissipate a power of up to 0.8 W, this transistor is appropriate to control the IRFP9140N MOSFET.

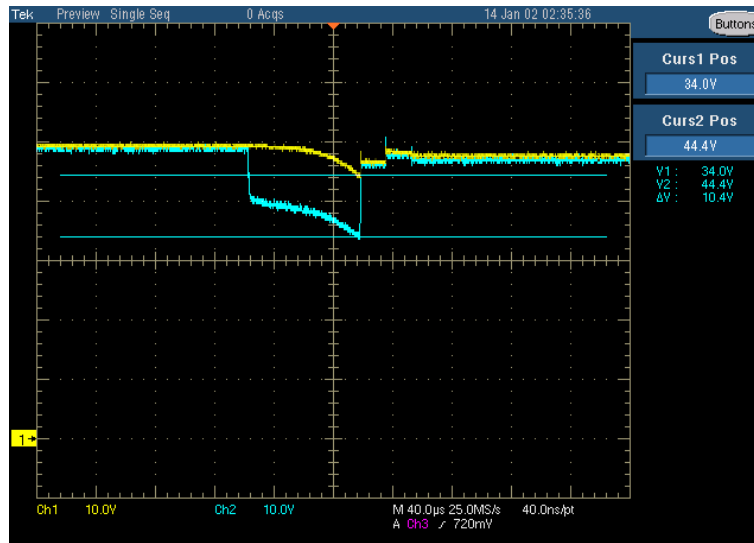


Figure 4.9: Voltage difference between Source and Gate on the IRFP9140N transistor

As seen in Figure 4.9, the voltage difference between source and gate is 10.4 V, approximately equal to the desired 10 V, and far from the maximum voltage that this MOSFET supports (20 V).



### **Battery selection**

During the maintenance period at the nominal current, the energy is directly supplied from the battery. For the 50 V selection, the used MOSFET is the IRF9140N model (P channel). This transistor has an antiparallel diode, as it is typical in the MOSFETs. In this work, this diode is a problem, since this can conduct the high voltage through it and then towards the battery. For this reason it has been necessary place another diode directly polarized between the transistor and the load.

In this case, by working always with a voltage less than 20 V between the source and the gate, the BJT 2N5551 that drives the MOSFET can enter in the saturation region.

For fast switching, it is necessary to quickly charge the gate capacitance. To this end the resistance between source and gate is 50  $\Omega$ .

#### **4.2.3.3 Current reading of the diesel injectors**

The current is measured by a resistance located between the voltage selection transistors and the loads. The voltage between terminals is amplified by the use of the AD8027 difference amplifier.

As a shunt is used a 10 m $\Omega$  resistor and the amplifier references tied to ground (Figure 4.10). When 20 A goes through the shunt, the voltage difference between its terminals is 200 mV. Being a 20 V/V gain, the output voltage of the amplified is 4 V. As the maximum input voltage of the microcontroller is 3.3 V, the voltage is then divided to the half by a voltage divider.

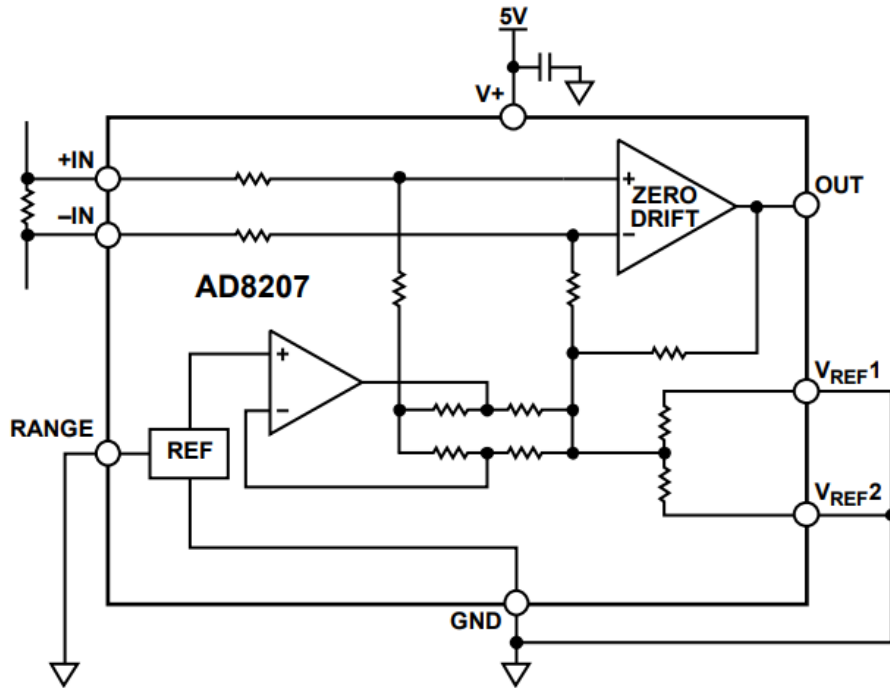


Figure 4.10: AD8207 Schematic. Ground Referenced Output Mode,  $V_+ = 5\text{ V}$ , [1]

#### 4.2.4 Selection of the injectors

The selection of the injectors is made by using a N-Channel MOSFET transistor, placed between the load and the ground. Here we meet the the problem that the output voltage of the microcontroller STM32 is 3.3 V and the current output up to 25 mA, that is too low to drive the MOSFET. For this reason it has been necessary to use a BJT transistor between the microcontroller and the MOSFET's gate. The schematic is shown in the Figure 4.11.

As already seen in the supply voltage selection, in order to obtain a fast switching, it is necessary to quick charge the gate capacitance, then a  $100\ \Omega$  resistance between source and gate was used.

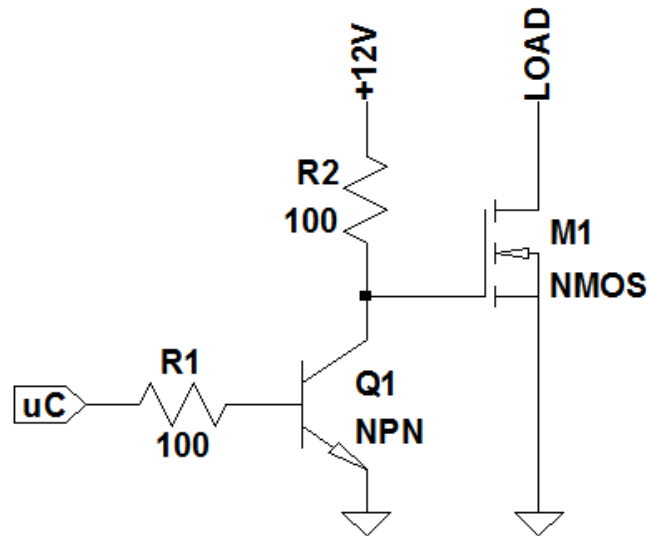


Figure 4.11: Low Side MOSFET driver

### 4.2.5 Acquisition of the trigger signal

All digital inputs of the STM32F401RE microcontroller are 5 V tolerant, which means that the input voltage can range between 0 and 5 V. The logic levels are defined by the range from 0 to  $0.1 \cdot V_{DD} + 0.1$  V for the low state, and from  $0.17 \cdot V_{DD} + 0.7$  to 5 V for the high state.

From 5.5 V upward the microcontroller is usually brought to a reset condition, while with higher values can also be broken. To avoid this, a two-level clipper circuit was placed between the motor signal and the microcontroller input pin, shown in Figure 4.12.

With this circuit, if the voltage exceeds 3.7 V, diode D1 is directly polarized, starting to drive and cutting the voltage signal. Similarly, if its value falls below -0.7 V, the diode D2 goes in conduction.

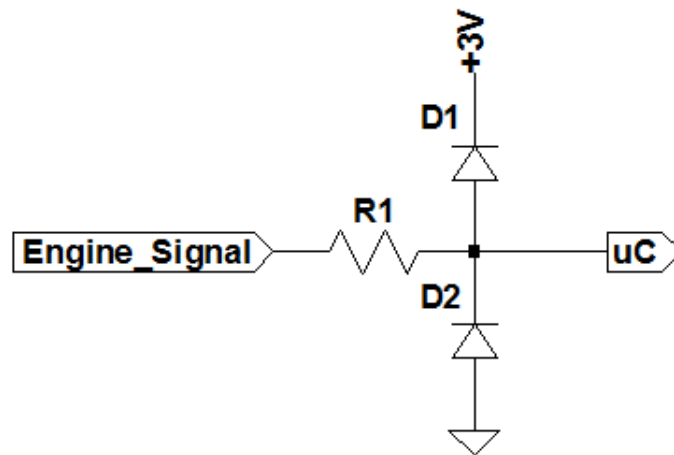


Figure 4.12: Conditioning of Trigger Signal

### 4.3 Microcontroller program

The control of the engine has been made by the generation of a series of signals to control the transistors that manage the injections and the charge of the boost converter according to the speed and position of the crankshaft and the current of diesel injectors.

The control sequence of diesel injection is as follows (Figure 4.14): when the timer indicates that the injection must to start, the selected injector's MOSFET closes. After this time the high voltage supply is selected. When the read current exceeds the preset value, the selector MOSFET opens, returning part of the energy to the converter. When the current arrives to the preset holding current, the current control starts.

The current control (Figure 4.15) is performed by acting both high and low side. In both sides, the current is controlled by a hysteresis controller. This control opens the MOSFETs when the current exceeds the preset value more a predefined gap, and closes them when the current decrease to the same preset value minus the gap.

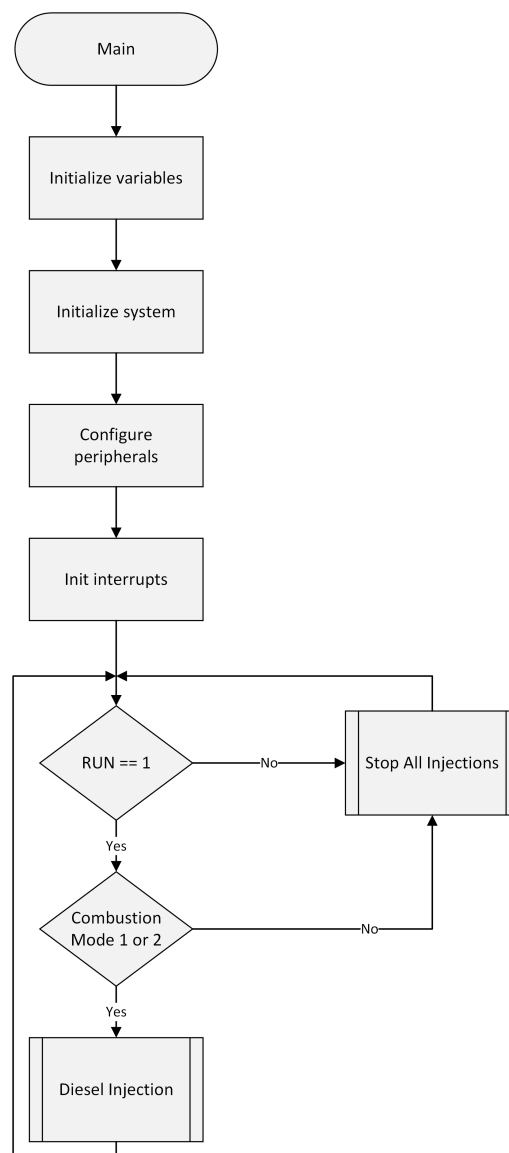


Figure 4.13: Main Flow Diagram

### 4.3.1 Calculation of the injection position

#### LPG-Diesel Mode

The calculation of the instant when fuel starts to be injected is performed once per cycle, just after detecting the falling edge of the trigger signal.

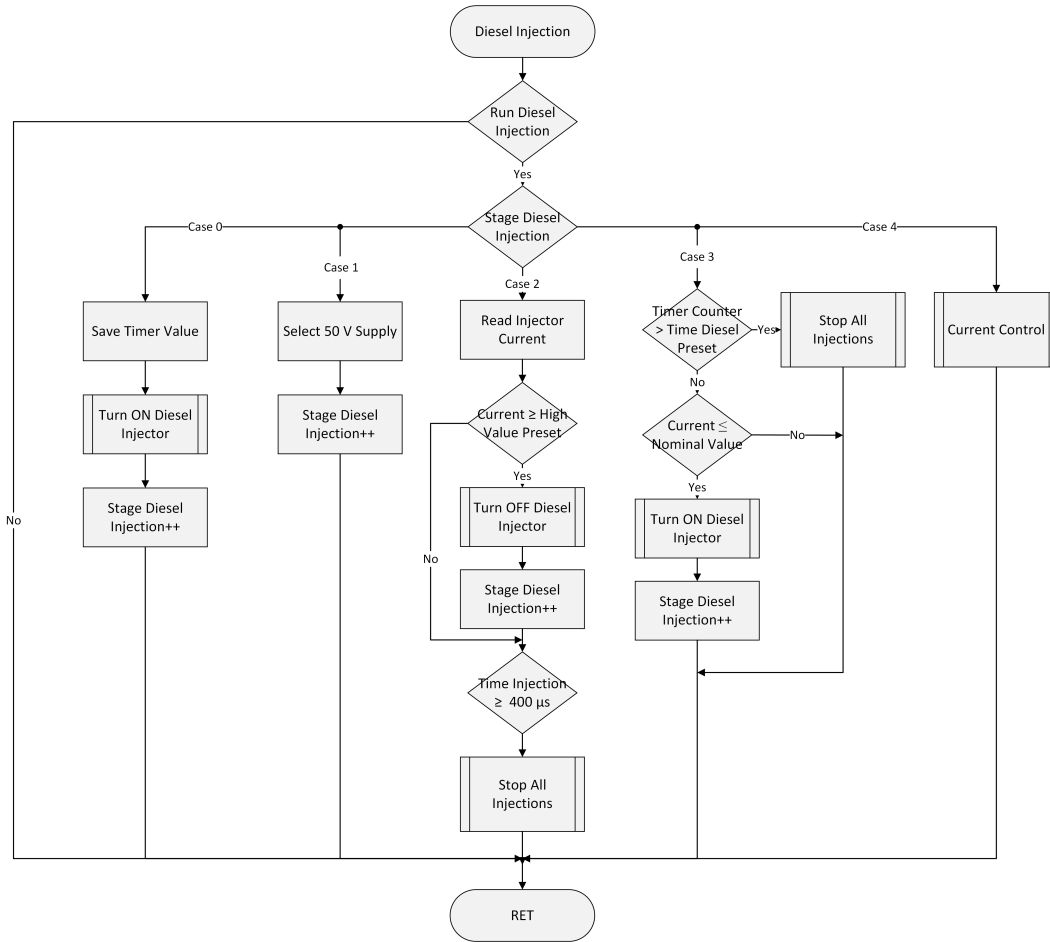


Figure 4.14: Diesel Injection Diagram

Firstly, the variation between the preset speed (2000 rpm) and the existing speed is calculated:

$$Time\ Relation = \frac{Engine\ Period\ Real}{Engine\ Period\ Preset\ (60\ ms)} \quad (4.11)$$

Then the end of the first injections at 2000 rpm are calculated:

$$LPG_{1(Final)} = \frac{Falling\ Edge\ (^{\circ}) - Ant.\ LPG\ Inj.\ (^{\circ})}{Engine\ Speed\ (rpm) \cdot \frac{360^{\circ}}{60\ s}} \cdot 1 \cdot 10^6 \quad (4.12)$$

$$Diesel_{3(Final)} = \frac{Falling\ Edge\ (^{\circ}) - Ant.\ Diesel\ Inj.\ (^{\circ}) - 240^{\circ}}{Engine\ Speed\ (rpm) \cdot \frac{360^{\circ}}{60\ s}} \cdot 1 \cdot 10^6 \quad (4.13)$$

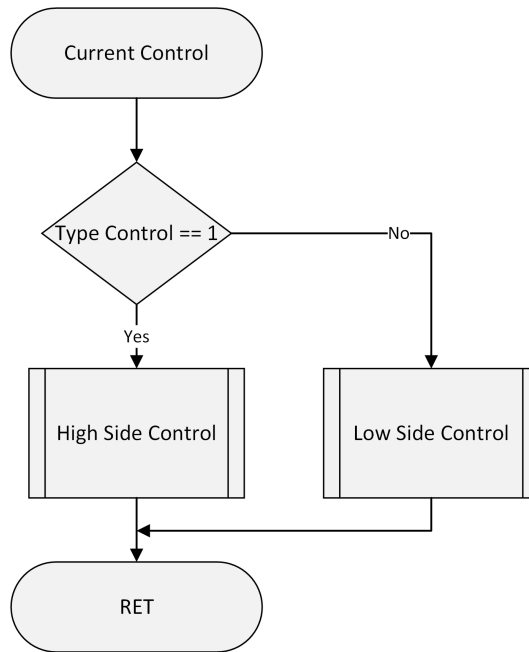


Figure 4.15: Current Control Diagram

Now the start time of the first gas injection is calculated with respect to the real engine speed:

$$LPG_{1(Init)} = LPG_{1(Final)} \cdot Time\ Relation - LPG\ Time \quad (4.14)$$

And the times between the remaining injections:

$$Diesel_{1,2\&3(Init)} = (Diesel_{3(Final)} - LPG_{1(Final)}) \cdot Time\ Relation - Diesel\ Time \quad (4.15)$$

$$LPG_{2\&3(Init)} = \frac{Engine\ Period}{3} - LPG\ Time - Diesel_{1,2\&3(Init)} - Diesel\ Time \quad (4.16)$$

These values are placed in the Autoreload Register of the timer each time that its interruption occurs.

### Conventional Diesel Mode

In this mode the steps are more or less the same, changing the LPG injections by the Diesel pre-injections:

Firstly, the variation between the preset speed and the existing is calculated. Then the ends of the first injections at 2000 rpm are calculated:

$$Pre. Diesel_{3(Final)} = \frac{Falling Edge (^{\circ}) - Ant. Pre. Diesel (^{\circ}) - 240^{\circ}}{Engine Speed (rpm) \cdot \frac{360^{\circ}}{60 s}} \cdot 1 \cdot 10^6 \quad (4.17)$$

$$Diesel Nom_{3(Final)} = \frac{Falling Edge (^{\circ}) - Ant. Nom. Diesel (^{\circ}) - 240^{\circ}}{Engine Speed (rpm) \cdot \frac{360^{\circ}}{60 s}} \cdot 1 \cdot 10^6 \quad (4.18)$$

Now the start time of the first pre-injection diesel is calculated with respect to the real engine speed:

$$Pre. Diesel_{1(Init)} = Pre. Diesel_{1(Final)} \cdot Time Relation - Pre. Diesel Time \quad (4.19)$$

And the times between the remaining injections:

$$Nom. Diesel_{1,2\&3(Init)} = (Nom. Diesel_{3(Final)} - Pre. Diesel_{1(Final)}) \cdot Time Relation - Diesel Time \quad (4.20)$$

$$Pre. Diesel_{2\&3(Init)} = \frac{Engine Period}{3} - Pre. Diesel Time - Nom. Diesel_{1,2\&3(Init)} - Diesel Time \quad (4.21)$$

These values are placed in the Autoreload Register of the timer each time that its interruption occurs.



### 4.3.2 Communication with the PC

The communication with the PC is performed through the UART peripheral. The operation is as follows, shown in Figure 4.16: The computer sends a string consisted in a letter (which selects the internal variable of the microcontroller to be modified) and a number (the value to modify). When a byte is received the execution is interrupted by the Rx Callback. Then the byte is saved in a char array. The last character received from the computer in each communication is the line feed (LF or \n). In this moment the string saved in the char array is decoded, placing the number received in the corresponding variable, as can be the injection time or the current level.

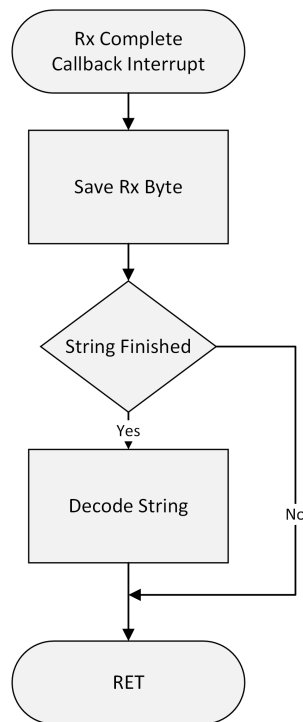


Figure 4.16: Communication Diagram

## 4.4 Virtual Instrument (LabVIEW)

The communication with the microcontroller was performed using the LabVIEW software. Within the VI program the dual-fuel or conventional combustion process can be chosen. Moreover changes in the current levels of the diesel injectors, or the time and position of each injection, can also be performed.

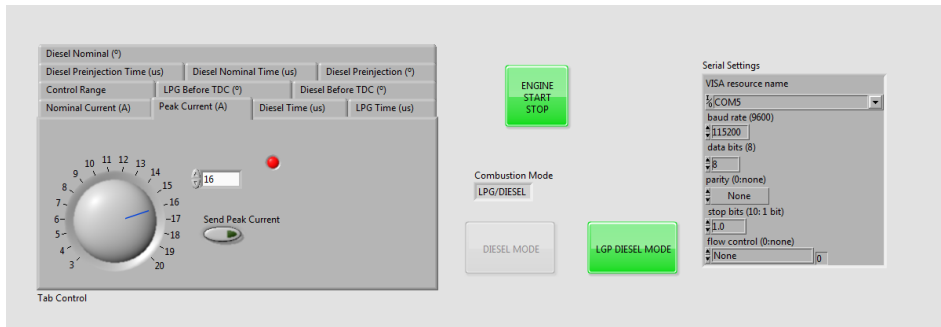


Figure 4.17: Front Panel of the Virtual Instrument

The communication parameters with the microcontroller are configured as follows:

- Baud rate: It is the data transfer speed measured in baud. The default value is 115200 baud (bit/s).
- Data bits: It is the number of bits sent. The default value is 8.
- Parity: It is used to verify errors in data transmission. By default it is not used.
- Stop bits: They are used to indicate the end of the transmission. They are necessary because each device has its own clock and they could not be synchronized. So these bits give a tolerance. By default only one bit is used.
- Flow control: It sets the type of control used in the transmission. Unused.
- Termination char: The read operation finishes when the termination char (LF by defect) is read.

## 4.5 Experimental measurements

In this last section will be exposed the time and current measurements of the injectors in both modes of operation (conventional diesel and dual fuel) obtained and displayed with the digital oscilloscope.

### 4.5.1 Conventional Diesel Fuel Injection

In conventional diesel mode, two injections per cycle are performed: an anticipated pre-injection of approximately  $400 \mu\text{s}$ , employed to establish the ideal conditions for the normal injection, of approximately  $600 \mu\text{s}$ . These times have been measured with the engine running at 1000 rpm.

In the Figure 4.18 the current that circulates through one of the engine injectors under the control of its original ECU can be observed.

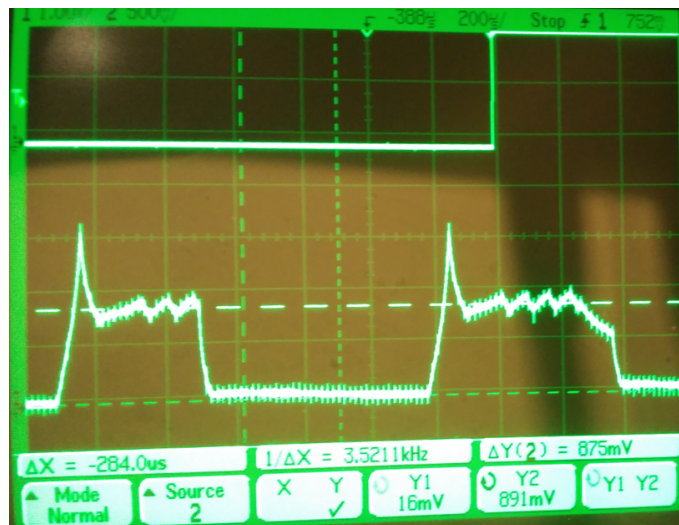


Figure 4.18: Solenoid-valve current (100 mV/A)

The measurements on the engine were obtained by a current clamp, with a output sensitivity of 100 mV/A. The peak current is 16 A and the holding current is 8.75 A

#### 4.5.1.1 Diesel injection controlled by the designed ECU

In the conventional diesel mode of operation it is required to be able to change the final fuel injection position and its duration with respect to the engine speed.

The following graphics have been obtained using a trigger signal, with 60 ms of period, by reference, equivalent to an engine operation at 2000 rpm.

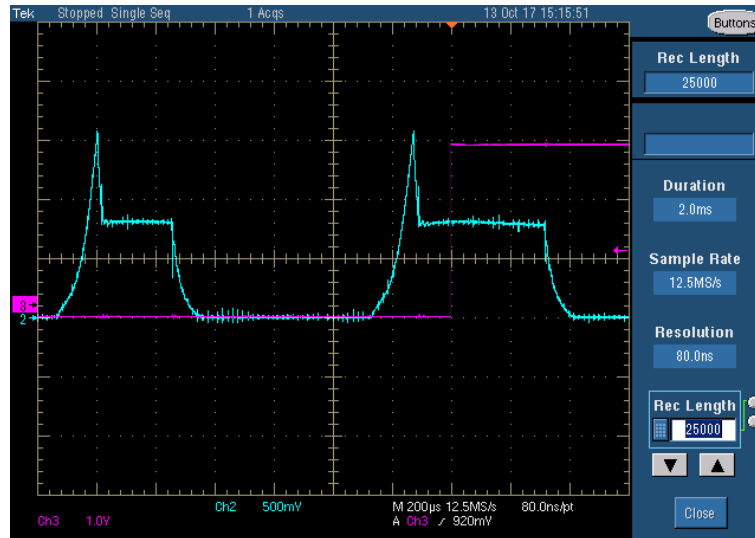


Figure 4.19: Solenoid current controlled by designed ECU (100 mV/A)

The waveforms show the current that goes through an inductive load of  $2\ \Omega$  y  $180\ \mu\text{H}$ , well simulating the real injector together the wires resistance, and reaching a current of 8 A.

The Figure 4.19 shows the pre-injection, which finishes  $15.5^\circ$  before the TDC, and the normal injection, which is anticipated only  $0.4^\circ$ . In the Figure 4.20 the pre-injection and the injection are anticipated  $20$  and  $10^\circ$  respectively, with the same duration as in the previous figure. The current is obtained by amplifying of the voltage drop in a shunt resistor.

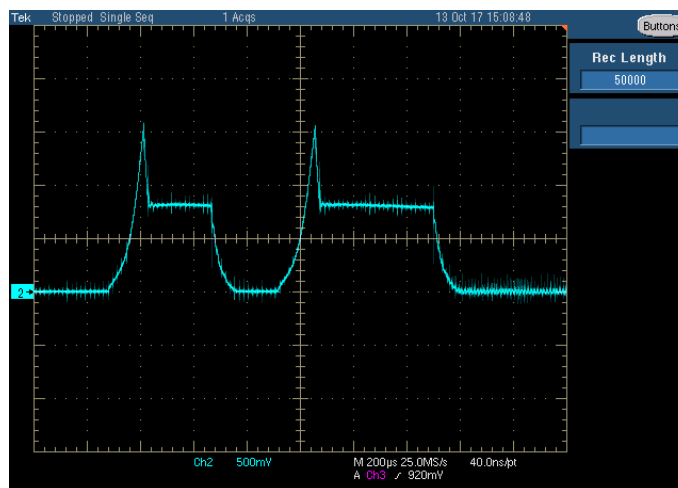


Figure 4.20: Solenoid-valve current (100 mV/A)

### 4.5.2 LPG-Diesel Fuel Injection

In the LPG-Diesel combustion mode, the gas fuel is injected at the start of the exhaust stroke in the inlet manifold,  $270^\circ$  before the TDC. It corresponds to 7.83 ms, at 2000 rpm and with the falling edge anticipated  $364^\circ$ . Since the gas injectors have not a current sensor, the voltage in the drain terminal has been considered in order to represent the injection.

The diesel injection in the same cylinder is done near the TDC in the Compression Stroke. In the Figure 4.22, the end of the injection is anticipated  $15^\circ$ .

In the Figure 4.23 the separation of  $240^\circ$  (20 ms at 2000 rpm) of crankshaft rotation between two consecutive injections of diesel is visible.

And in the Figure 4.24 it can be observed the current that goes through one of the diesel engine injector, injection anticipated  $10^\circ$ . Due to the resistance of the wires the system does not need to control the current.

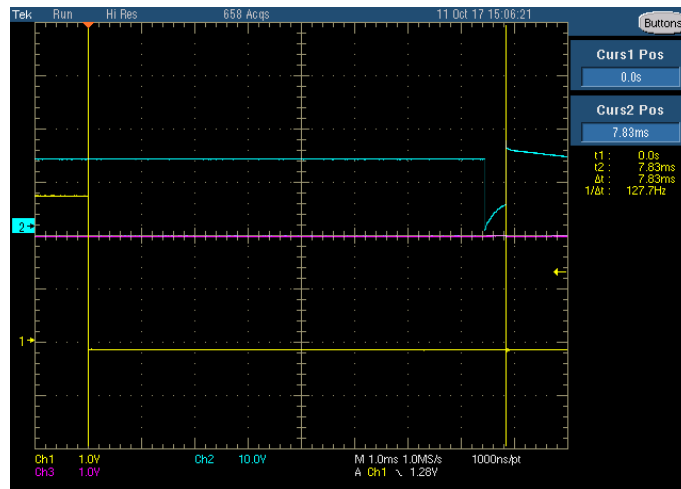


Figure 4.21: LPG injection at 2000 rpm

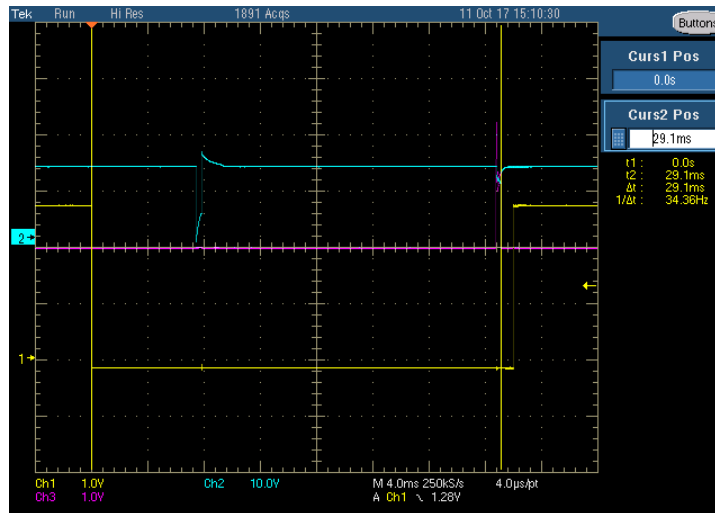


Figure 4.22: Diesel injection at 2000 rpm

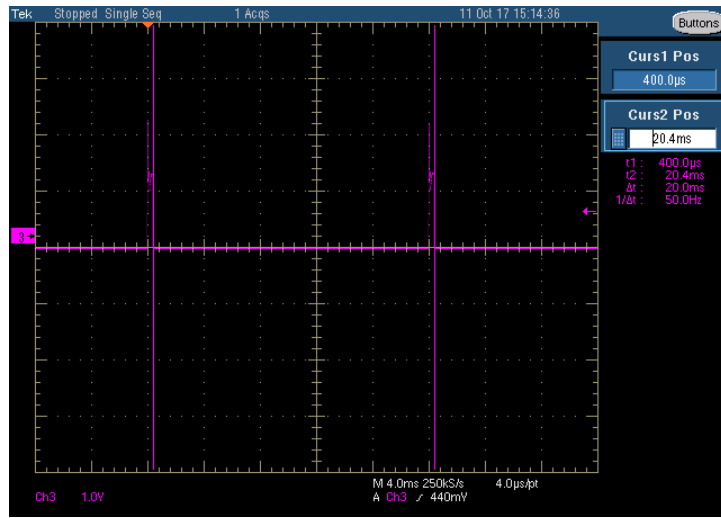


Figure 4.23: Separation between diesel injections (2000 rpm)

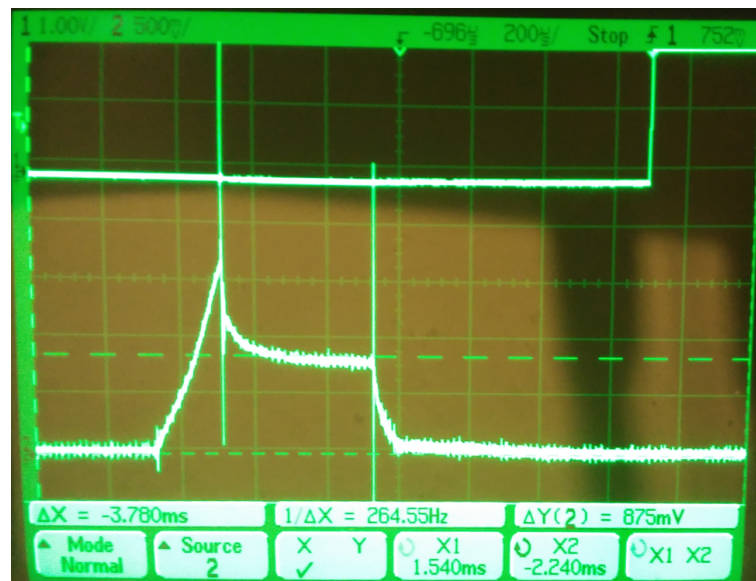


Figure 4.24: Solenoid-valve current controlled by designed ECU (100 mV/A)





## 5 Conclusion

Throughout this work an Engine Control Unit for the management of a LPG-Diesel dual-fuel engine has been designed and implemented, capable of work with diesel only or a combination of diesel and gas.

The ECU has been made using the STM32 NUCLEO-F401RE development board which, attached to a designed and built tailored daughter board which acts as final stage, is capable to sample the crankshaft engine signal and the current that goes through the diesel injectors to control the time and shape of the injection signals, generating the proper outputs to control the engine under test.

By the use of the virtual instrument running as LabVIEW application through a personal computer is able to choose between the two different operation modes, diesel only and dual fuel, being able to change the position and time of each injection.

Therefore, thanks to the work accomplished, a system able to control the engine in both operating modes has been created.



# Bibliography

- [1] Analog Devices. *Datasheet: AD8207 - Zero-Drift, High Voltage, Bidirectional Difference Amplifier*, 2010.
- [2] H. Bendu and S. Murugan. Homogeneous charge compression ignition (HCCI) combustion: Mixture preparation and control strategies in diesel engines, challenges and solutions. *Renewable and Sustainable Energy Reviews*, 57:282–291, 2016.
- [3] J. E. Dec. Advanced compression-ignition engines — understanding the in-cylinder processes. *Proceedings of the Combustion Institute*, 32:2727–2742, 2009.
- [4] M. Farrugia, C. Seychell, S. Camilleri, G. Farrugia, C. Caruana, and M. Farrugia. Diesel engine control strategy for a programmable engine control unit. *International Journal of Sciences and Techniques of Automatic control & computer engineering*, 10:2062–2071, 2016.
- [5] M. M. Hasan and M. M. Rahman. Homogeneous charge compression ignition combustion: Advantages over compression ignition combustion, challenges and solutions. *Renewable and Sustainable Energy Reviews*, 57:282–291, 2016.
- [6] J. B. Heywood. *Internal Combustion Engine Fundamentals*. McGraw-Hill, Inc, 1988.
- [7] KOHLER Engines. *KDI 1903 TCR - KDI 2504 TCR Manuale Officina*.

- [8] Linear Technology. *Datasheet: LTC1871 - High Input Voltage, Current Mode Boost, Flyback and SEPIC Controller*, 2002.
- [9] X. Lu, D. Han, and Z. Huang. Fuel design and management for the control of advanced compression-ignition combustion modes. *Progress in Energy and Combustion Science*, 37:741–783, 2011.
- [10] F. Payri and J. M. Desantes. *Motores de combustión interna alternativos*. Editorial Universitat Politècnica de València, 2011.
- [11] K. Reif. *Diesel Engine Management*. Springer Vieweg, 2014.
- [12] K. Reif. *Fundamentals of Automotive and Engine Technology*. Springer Vieweg, 2014.
- [13] STMicroelectronics. STM32F401RE - STM32 Dynamic Efficiency MCU, ARM Cortex-M4 core with DSP and FPU, up to 512 Kbytes Flash, 84 MHz CPU, Art Accelerator [Online]. [www.st.com/en/microcontrollers/stm32f401re.html](http://www.st.com/en/microcontrollers/stm32f401re.html). Accessed: 28-09-2017.
- [14] STMicroelectronics. SW4STM32 [Online]. [www.st.com/en/development-tools/sw4stm32.html](http://www.st.com/en/development-tools/sw4stm32.html). Accessed: 24-08-2017.
- [15] STMicroelectronics. *Application note: AN3116 - STM32<sup>TM</sup>'s ADC modes and their applications*, 2010.
- [16] STMicroelectronics. *Datasheet: STM32F401xD STM32F401xE*, 2015.
- [17] STMicroelectronics. *Application note: AN4013 - STM32 cross-series timer overview*, 2016.
- [18] STMicroelectronics. *DataBrief: NUCLEO-XXXXRX STM32 Nucleo-64 board*, 2016.

- [19] STMicroelectronics. *DataBrief: STMCubeF4 - STM32Cube embedded software for STM32F4 Series including HAL, low-layer drivers and STM32F4-dedicated middleware*, 2017.
- [20] STMicroelectronics. *User manual: UM1718 - STM32CubeMX for STM32 configuration and initialization C code generation*, 2017.
- [21] STMicroelectronics. *User manual: UM1725 - Description of STM32F4 HAL and LL drivers*, 2017.